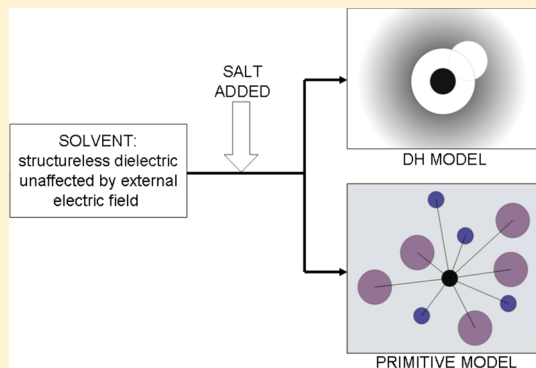


# Computing Excess Functions of Ionic Solutions: The Smaller-Ion Shell Model *versus* the Primitive Model. 1. Activity Coefficients

Dan Fraenkel\*

Eltron Research &amp; Development Inc., 4600 Nautilus Court South, Boulder, Colorado 80301-3241, United States

**ABSTRACT:** The present study compares the Monte Carlo (MC) simulation of the primitive model (PM) (Abbas, Z. et al. *J. Phys. Chem. B* **2009**, *113*, 5905), by which activity coefficients of many binary ionic solutions have been computed through adjusting ion-size parameters (ISPs) for achieving best fit with experiment, with a parallel fit and ISP adjustment, employing the Smaller-Ion Shell (SiS) treatment (Fraenkel, D. *Mol. Phys.* **2010**, *108*, 1435), a Debye–Hückel type theory (“DH–SiS”) considering counterions of unequal size. DH–SiS is analogous to the unrestricted PM (UPM), so the comparison is with the MC simulation of the UPM, “MC–UPM”. Among the representative electrolytes NaCl, KCl, NaClO<sub>4</sub>, CaCl<sub>2</sub>, Ca(ClO<sub>4</sub>)<sub>2</sub>, and LaCl<sub>3</sub>, in water at 25 °C, the 1–1 electrolytes exhibit a far better fit quality for DH–SiS than for MC–UPM, and the fit extends to higher concentration. Moreover, theoretical single-ion activity coefficients derived from DH–SiS agree with experimental estimation for solutions of NaCl, CaCl<sub>2</sub>, and other electrolytes (Fraenkel, D. *J. Phys. Chem. B* **2012**, *116*, 3603), whereas parallel MC–UPM predictions are at odds with experiment. Additional advantages of DH–SiS over MC–UPM are in (a) employing co-ion ISPs that are usually equal to the crystallographic ion diameters and (b) easily applying ISP nonadditivity in adjusting counterion ISPs.



## 1. INTRODUCTION

Over the past half century, many advanced theories have been developed to allow better understanding of the physicochemical behavior of electrolyte solutions;<sup>1</sup> such theories were aimed at computing excess thermodynamic functions more effectively and at correlating these functions more straightforwardly with the electrolyte valence family, ion size, and concentration (or ionic strength).

The major starting point in the development of advanced ionic theories since 1960 has been the primitive model (PM).<sup>2</sup> The PM considers ions as positively and negatively charged hard spheres immersed in a structureless dielectric continuum that is assumed to be unaffected by the strength of an electric field exerted on it. The system is characterized by a critical interionic distance (“distance of closest approach”),  $R_{ij}$ ,  $i$  and  $j$  denoting any two mutually approaching ions. The interaction potential between the ions,  $u_{ij}$ , is infinite at  $r < R_{ij}$ ,  $r$  being the radial distance from the reference ion center (“origin”), and at  $r \geq R_{ij}$  it is equal to the coulomb potential,  $q_i q_j / \epsilon r$ ,  $q$ 's being the respective charges of the ions and  $\epsilon$ , the medium's permittivity.

If  $i$  and  $j$  denote different types of ions in a binary system—say  $i$  is the positive ion,  $j$  the negative—then there are three distances of closest approach, or ion-size parameters (ISPs),  $R_{ii}$ ,  $R_{jj}$ , and  $R_{ij}$ , which represent, respectively, the mutual approach of the  $i$ – $i$ ,  $j$ – $j$ , and  $i$ – $j$  ions. In the PM, the  $R$ 's are obviously additive,<sup>2</sup> so  $R_{ij}$  ( $= R_{ji}$ ) =  $(R_{ii} + R_{jj})/2$ . If all  $R$ 's are equal, the PM, with a single ISP, “ $R$ ”, is called the “restricted primitive model,” RPM; otherwise, it is referred to as the “unrestricted primitive model,” UPM.

Excess functions, such as osmotic and activity coefficients, can be computed by Molecular Dynamic (MD) or Monte Carlo (MC) simulations of the PM.<sup>3–5</sup> PM-based theories of excess functions result in complicated mathematical expressions based on advanced integral equations (e.g., Percus–Yevick and Ornstein–Zernike equations<sup>1</sup>) that can only be solved numerically. The validity of an advanced theory has been normally examined against MC simulations of the PM. Thus, the general literature view has been that under conditions at which MC simulations accurately reflect the model, here the PM (i.e., not at too dilute solutions and not considering in the computation too small numbers of ions), theories only need to replicate the *simulated* excess functions.

So far, only sporadic studies have been published in which MC simulations of the PM or integral equation theories were compared with experimental excess functions. To draw an unequivocal conclusion on the agreement of the PM with experiment, more extensive simulation studies had to be performed, covering a large number of electrolytes of various valence families and having ions of different sizes, at broad concentration ranges. Through this, “mapping” of the intrinsic overall behavior of electrolyte solutions could be achieved. In the current context, “mapping” implies consistency examination by covering a “field” of various electrolyte families and solution conditions and a sufficient number of individual cases of binary ion systems. This challenge was undertaken a few years ago by

Received: July 31, 2014

Published: November 4, 2014

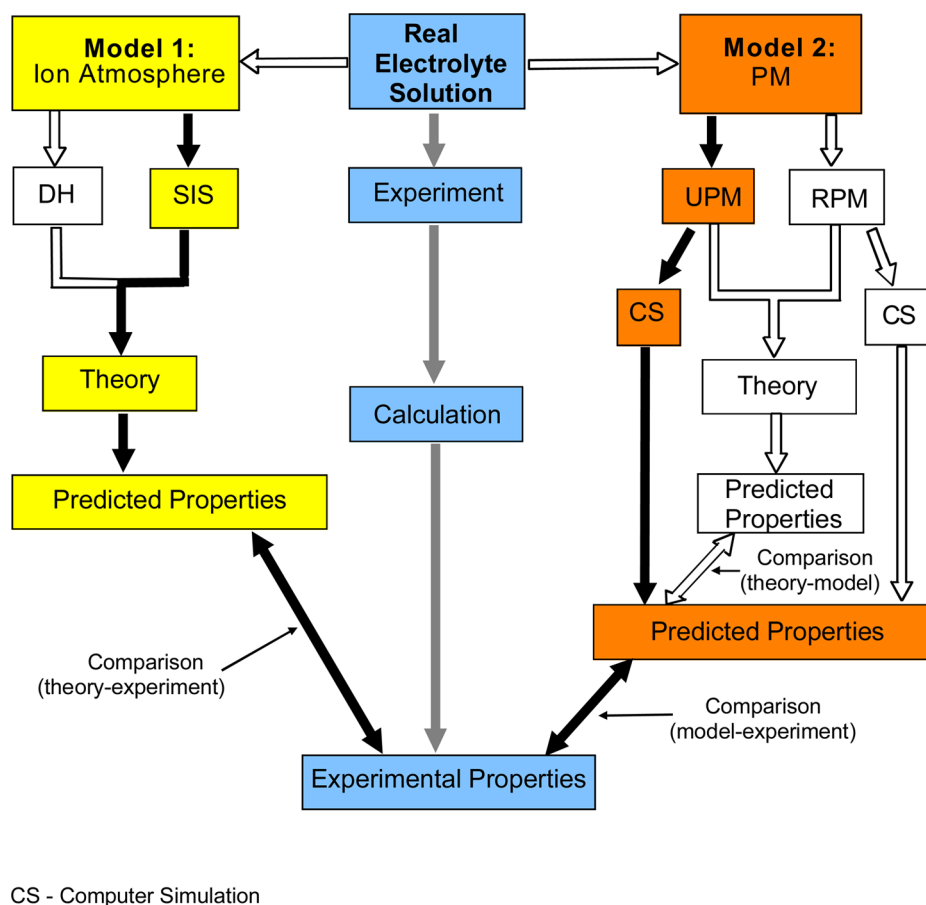


**Figure 1.** A model–theory–experiment relationship diagram (after Allen, M. P.; Tildesley, D. J. *Computer Simulations of Liquids*; Clarendon Press: Oxford, 1987) for electrolytes in solution. Full dark arrows represent pathways followed in the current study—on the right, the pathway represents a “model test”; on the left, a “theory test”. Open arrows (and open boxes) are literature pathways that are not considered in the current study. A successful theory implicitly indicates a successful model on which the theory is based. An unsuccessful theory may result from deficiencies in either the theory or its model. An unsuccessful model (judged by bad model–experiment comparison) causes all theories based on it to be doomed. Therefore, a theory–model comparison (open arrows and open boxes on the right) is not sufficient for judging the success of either the theory or its model. In the diagram, yellow boxes represent the electrostatic DH-type route (“Model 1”), and orange boxes represent the PM, as UPM (“Model 2”). Blue boxes represent the experiment. Predicted Properties (i.e., excess functions) by both Model 1 and Model 2 are compared with Experimental Properties. Such a comparison may distinguish one model from the other in regard to the effectiveness of producing the properties as derived from experiment (see text for details).

Abbas et al.<sup>6</sup> who have devoted an entire study to extensive MC simulations of the PM aimed at achieving “best fit” of the PM with experiment (osmotic and activity coefficients vs concentration) via ISP optimization.

Here, I examine the above study and the interpretation of its results; restricting this to the UPM, I denote the model MC–UPM. I further restrict the examination to the activity coefficient and its dependence on ionic strength. I compare the MC–UPM simulated data with computations of parallel electrolyte systems, using equations of the Smaller-ion Shell (SiS) treatment.<sup>7,8</sup> The SiS treatment is an extension of the Debye–Hückel (DH) theory<sup>9–13</sup> (hence dubbed DH–SiS) for counterions of unequal size. Due to the size-dissimilarity, an atmospheric shell exists around each “chosen ion”, which accommodates only the smaller atmospheric ions. In DH–SiS, this shell is incorporated *straightforwardly* into the DH model.<sup>7,8</sup> The resultant model–theory development is somewhat more elaborate than that of the DH theory, but it is still simple and tractable, providing an analytic mathematical solution. DH–SiS affords a better theory–experiment fit than the parent DH model.<sup>7,8</sup> Inasmuch as the DH model pertains to

the general realm of the RPM, DH–SiS is set in the framework of the UPM; however, *neither model is built upon the PM*.

The distinction between DH–SiS and the PM is further illustrated in Figures 1 and 2. The major differences are outlined below.

1) **ISP additivity.** Unlike the PM, DH–SiS is not a “hard-spheres’ model” hence there is no *a priori* requirement of ISP additivity. This is crucial since ISP nonadditivity reflects the very nature of real electrolytes, resulting from the different electronic factors playing a role when an ion is approached by different types of ions (e.g.,  $\text{Cl}^-$  approached by  $\text{Cl}^-$  or by  $\text{Na}^+$  in aqueous NaCl).

2) **Ion–ion interaction.** In the PM, all ions are treated as “equal-right” members of the ion assembly in solution, each with size and volume and identical to any other co-ion. Although being a many-body type model, the PM considers only two-body (pairwise) potentials.<sup>2,14</sup> Thus, any ion in the PM interacts with all other ions but only in a “one-on-one” fashion; no three-ion or higher-level multi-ion potentials are accounted for. Including such potentials would render the PM very complex, and computations, e.g., MC simulations, would

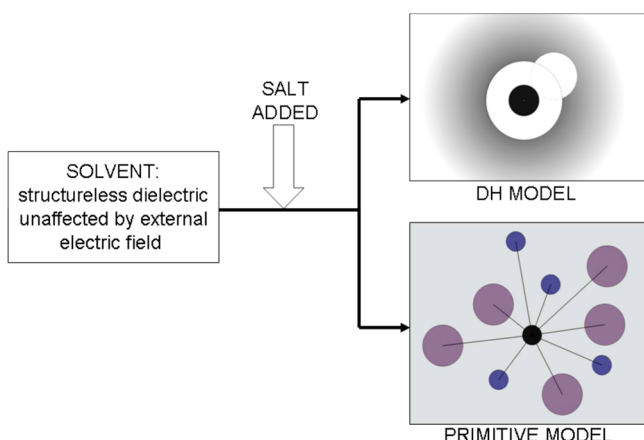


**Figure 2.** Differences between the DH model and the primitive model (PM): Dissolving a salt in a solvent leads to two different “pictures” describing how ions “see” one another in the McMillan–Mayer (MM) realm and, consequently, how they interact in solution. In the DH model, a central ion (black full circle in the middle) is surrounded by its ionic atmosphere (charge density of all other ions as electric point charges, presented as shaded area), with a spherical border (“rim”) corresponding to the distance of closest approach of the central ion to an atmospheric ion (colorless open circle) whose center defines the rim. The central ion interacts with its ionic atmosphere considered as a spherically symmetric integral ionic entity. In the PM, a chosen ion (middle black sphere) interacts pairwise with “all” surrounding ions—co-ions (blue spheres) and counterions (purple spheres).

then require much more computer capacity and time. It is generally believed that the higher-level interionic potentials do not contribute substantially to the PM. In the DH model, in contrast, there are only two mutually interacting “electrostatic entities” — a central (“chosen”) ion and its surrounding ionic atmosphere (or “cloud”) (Figure 2). Therefore, conceptually, there is no loss of interaction potential due to not considering potential terms of multi-ions, and “all other ions” are lumped in the charge distribution of the ionic atmosphere. The McMillan–Mayer (MM) formalism<sup>15</sup> and Mayer’s theory of electrolytes<sup>16</sup> ensure us that for computing excess functions, at the microscopic level, in a sufficiently dilute solution, all we need is an effective potential,  $w_{ij}^{\circ}(r)$ , and not the real, physically accurate potential,  $u_{ij}(r)$ .<sup>5</sup>

3) **Potential at  $r \leq a$ .** Furthermore, unlike the PM, the DH model does not assume infinite potential at  $r \leq R_{ij}$  (or  $R$ ) (see above). The electrostatic potential in the spherical shell bordered by the radii of the cloud edge (“rim”) and of the central ion, at which the charge density of cloud ions is zero, is chosen as the self-potential of the central ion. This is not zero, nor is it infinity. In the PM, ion collisions occur between two “equal-right” ions carrying their respective full charges, even though the interaction potential between those ions is screened by the other surrounding ions. In contrast, the “collision” in the DH model is between the central ion ( $\beta$  ion), as a “full ion” having its entire electric charge, and an atmospheric ion ( $\alpha$  ion), as a “partial ion” residing on the cloud rim. This quasi-ion brings only a small portion of the cloud’s charge to the interaction because of the broad spread of this charge over the entire ionic atmosphere.<sup>8</sup>

4) **Poisson–Boltzmann equation vs advanced integral equations.** In addition to not being a PM according to the conventional definition, the DH model is treated mathematically not by an advanced integral equation but by the Poisson–Boltzmann (PB) equation. Two major approximations are

believed to limit the effectiveness of the DH theory, compared with the (perceived) effectiveness of PM-based theories using advanced integral equations or even cluster expansion techniques:<sup>17,18</sup> (a) The PB equation is commonly used in its linearized form, which is only justified when the average electrostatic potential is considerably smaller than the kinetic energy,  $kT$  ( $k$ , Boltzmann constant;  $T$ , absolute temperature). The electrolyte concentration range at which the linearization is physically and mathematically suitable depends on the choice of the criterion for “average electrostatic interaction potential” between the ions. (b) The DH theory applies a field-average potential of ionic interaction; modern theories use, instead, the statistical-mechanically more accurate force-average potential.<sup>2</sup> It is unclear, though, how the difference between those two types of average potential influences the overall outcome of model development, as judged by theory–experiment agreement at low-to-moderate ionic concentration.

Thus, besides not being based on the PM, the DH theory (and DH–SiS) uses nonrigorous statistical-mechanical tools and quite aggressive approximations; the physically “accurate” theories, such as the hypernetted chain (HNC) equation,<sup>19</sup> are based on the PM, and they are accurate in the sense of being capable of almost precisely reproducing the simulated thermodynamic data (excess functions), that is, those data directly emanating from the *model itself*; see Figure 1. At this point, two questions should be asked: (1) Does the PM effectively represent actual electrolytes in solutions? (2) Is the DH theory, despite its mathematical-physical “shortcuts”, capable of reflecting the essence of real electrolytes, even if compromising high accuracy, at least up to moderately concentrated solutions? The current study attempts to answer these questions through a close comparison between MC–UPM and DH–SiS and their fit with experiment.

The MC–UPM/DH–SiS model comparison study reported here is divided into two parts: The present article (Part 1), in which I scrutinize the fit of theory (or model) with experiment in regard to fit quality and fit range, by examining six representative electrolytes; and the subsequent article (Part 2, DOI 10.1021/ct500694u), in which I specifically examine ISPs of theory–experiment best fit, in both MC–UPM and DH–SiS, for their physicochemical validity and meaning.

## 2. MODELS AND METHODS

**2.1. MC–UPM versus DH–SiS.** The Monte Carlo (MC) simulations of the primitive model were done by Abbas et al.<sup>6</sup> using the standard Metropolis algorithm, and activity coefficients were derived from a modified Widom’s particle insertion method,<sup>20</sup> according to which

$$\ln \gamma = -\ln \left\langle \exp \left[ -\frac{\Delta U_{\alpha}(r)}{kT} \right] \right\rangle_0 \quad (1)$$

$\gamma$  is the activity coefficient of a nonperturbing particle  $\alpha$  inserted at a random position  $r$ , and  $\Delta U_{\alpha}$  is the ensemble average of the potential energy change, at  $r$ , due to the addition of particle  $\alpha$ . Re-establishing charge neutrality in the cubic cell was done<sup>6</sup> using the Svensson–Woodward charge rescaling method.<sup>21</sup> The fit with experiment was obtained<sup>6</sup> by optimizing ISPs simultaneously for the activity and osmotic coefficients.

DH–SiS is an electrostatic theory.<sup>7</sup> The size-dependent extra electrostatic potential energy of ionic interaction is different for the smaller ( $s$ ) and larger ( $l$ ) ions. The activity coefficient of the chosen  $i$  ion,  $\gamma_i$ , at sufficiently dilute solution, is approximated as

its part relating to the electrical energy. Through a “charging process”,  $\gamma_i$  is correlated with the field-average extra electrostatic energy per unit charge,  $\Psi_i$ , by

$$\ln \gamma_i \left( = \frac{\mu_{i,el}}{kT} \right) = \frac{1}{2} z_i^2 \Psi_i \quad (2)$$

$\mu_{i,el}$  is the electrical part of the chemical potential of the  $i$  ion with a charge  $z_i$ . The expression for the *mean ionic activity coefficient*,  $\gamma_{\pm}$ , in a binary electrolyte system, when the charge of the positive ion is  $z_+$  and that of the negative ion is  $z_-$ , is

$$\ln \gamma_{\pm} = \frac{1}{2} |z_+ z_-| \Psi_{\pm} \quad (3)$$

in which  $\Psi_{\pm}$  is defined (in analogy to  $\ln \gamma_{\pm}$ ) as

$$\Psi_{\pm} \equiv \frac{1}{z} \sum_{i=+, -} |z_i| \Psi_i; \quad z = \sum_{i=+, -} |z_i| \quad (4)$$

The  $s$ - and  $l$ -ions can each be positive or negative, so an  $(s, l)$  set is either  $(+, -)$  or  $(-, +)$ . Considering the electroneutrality condition,  $\sum_{i=+, -} z_i \nu_i = 0$ , eq 4 can be written as

$$\Psi_{\pm} = \frac{1}{z} \sum_{i=s, l} |z_i| \Psi_i = \frac{1}{\nu} (\nu_l \Psi_s + \nu_s \Psi_l) \quad (5)$$

$\nu_s$  and  $\nu_l$  being, respectively, the multiplicities of the  $s$ - and  $l$ -ions in the electrolyte “molecular” formula, and  $\nu_s + \nu_l = \nu$  ( $= \nu_+ + \nu_-$ ). Combining eq 5 with 3, we get

$$\ln \gamma_{\pm} = \frac{1}{2\nu} |z_+ z_-| (\nu_l \Psi_s + \nu_s \Psi_l) \quad (6)$$

and the calculation of  $\gamma_{\pm}$  vs  $I$  (ionic strength) only requires finding appropriate expressions<sup>7</sup> for  $\Psi_s$  and  $\Psi_l$  as functions of the reciprocal screening length,  $\kappa$  ( $= \mathcal{B} I^{1/2}$ )<sup>22</sup> and the ISPs.

**2.2. The Molar and Molal Scales and Their Inter-conversion.** The PM is based on the Lewis–Randall (LR) molal system, but MC simulations are more conveniently performed in the McMillan–Mayer (MM) molar system.<sup>6</sup> Therefore, in the Supporting Information of ref 6 (“Supporting Information Available”), the MC simulation provides the molar activity coefficient  $y_{\pm}$  (denoted  $\gamma_{\pm}$  in ref 6) against  $M$ ; along with  $y_{\pm}$ , the individual ionic activity coefficients,  $y_+$  and  $y_-$  (“ $\gamma_+$ ” and “ $\gamma_-$ ” in ref 6) are also presented. To examine the MC–UPM values ( $y_{\pm}$ ,  $y_+$ ,  $y_-$ ) versus concentration against the experimental behavior, the corresponding  $\gamma_{\pm}$ -vs- $m$  data of the experiment, that is, molal activity coefficient vs molality, have been converted to  $y_{\pm}$ -vs- $M$  data (see Appendix A). This has been done here to form a coherent basis for the current comparison, since converting the computed values of Abbas et al.<sup>6</sup> to the LR system is unfeasible.

For the same kind of comparison of experiment with DH–SiS, calculated activity coefficients in the MM system against molar concentration (or “molar  $I$ ”,  $I_v$ )<sup>12</sup> were obtained from the SiS equations,<sup>8</sup> assuming  $b_s = b_+$ ,  $b_l = b_-$ ,  $z_s = z_+$ , and  $z_l = z_-$

$$\log y_+ = -z_+^2 \frac{\mathcal{A}}{\mathcal{B}} \times \frac{\kappa}{1 + \kappa a} \times \left\{ 1 - \frac{2 \exp[\kappa(a - b_+)] - \kappa(a - b_+) - 2}{1 + \kappa b_+} \right\} \quad (7)$$

$$\log y_- = -z_-^2 \frac{\mathcal{A}}{\mathcal{B}} \times \frac{\kappa}{1 + \kappa a} \times \left\{ 1 + \frac{2 \exp[\kappa(b_- - a)] - 2\kappa(b_- - a) - 2}{1 + \kappa b_-} \right\} \quad (8)$$

and, considering that  $\nu \log y_{\pm} = \nu_+ \log y_+ + \nu_- \log y_-$

$$\log y_{\pm} = -|z_s z_l| \frac{\mathcal{A}}{\mathcal{B}} \times \frac{\kappa}{1 + \kappa a} \times \left\{ 1 - \frac{\nu_l}{\nu} \times \frac{2 \exp[\kappa(a - b_s)] - \kappa(a - b_s) - 2}{1 + \kappa b_s} + \frac{\nu_s}{\nu} \times \frac{2 \exp[\kappa(b_l - a)] - 2\kappa(b_l - a) - 2}{1 + \kappa b_l} \right\} \quad (9)$$

In eqs 7–9,  $\mathcal{A}$ ,  $\mathcal{B}$ , and  $\kappa$  – the standard parameters of the DH theory<sup>22</sup> – are in the MM system; in water at 25 °C,  $\mathcal{A} = 0.51077$  (liter-solution/mol-solute)<sup>1/2</sup>, and  $\mathcal{B} = 0.0032897$  pm<sup>-1</sup>(liter-solution/mol-solute)<sup>1/2</sup>.

The ISPs  $a$ ,  $b_+$ , and  $b_-$  substitute  $R_{ij}$  ( $= R_{ji}$ ),  $R_{ib}$  and  $R_{jl}$ , respectively, for the case  $R_{ii} < R_{ij}$  (see the Introduction section). Thus, ISP additivity requires the equality  $a = (b_+ + b_-)/2$ . A nonadditivity factor,  $d$ , is defined as  $d \equiv 2a - b_+ - b_-$ , and “percent nonadditivity” is defined as  $100d/(b_+ + b_-)$ , which is the percent departure of  $a$  from the sum  $1/2b_+ + 1/2b_-$ , relative to this sum. DH–SiS computations of activity coefficients, based on eqs 7–9, were performed as described in detail previously.<sup>7,8</sup>

In converting the DH parameters  $\mathcal{A}$ ,  $\mathcal{B}$ , and  $\kappa$  from molal to molar basis, I have used the relation<sup>8,12</sup>  $I_v \approx \sigma I_w$  where  $\sigma$  is the density of water, and subscripts  $v$  and  $w$  denote volume and weight basis. The relation holds at low concentration, up to  $\sim 1$  M( $m$ ),<sup>8</sup> but is still effective at higher concentration when the solution density is not much higher than the density of the solvent (water). The LR  $\rightarrow$  MM conversion increases the activity coefficient values at the same nominal electrolyte concentration, and the extent of this increase becomes gradually greater as the concentration is raised; but the declining  $\varepsilon$  of the solution as a function of concentration counteracts this effect, causing data in the LR system with  $\varepsilon$  of the solvent to be close to activity data in the MM system with  $\varepsilon$  of the solution. Nevertheless, in MC–UPM  $\varepsilon$  was chosen as that of the solvent<sup>6</sup> so it is imperative, for consistency, to use the solvent’s  $\varepsilon$  also in the DH–SiS calculation as provided here. It is noteworthy that the change from the LR to the MM system, keeping  $\varepsilon$  as that of the solvent, results in about the same fit quality in both cases, and the fit is gained with similar ISPs, as demonstrated for DH–SiS in Part 2 (DOI 10.1021/ct500694u).

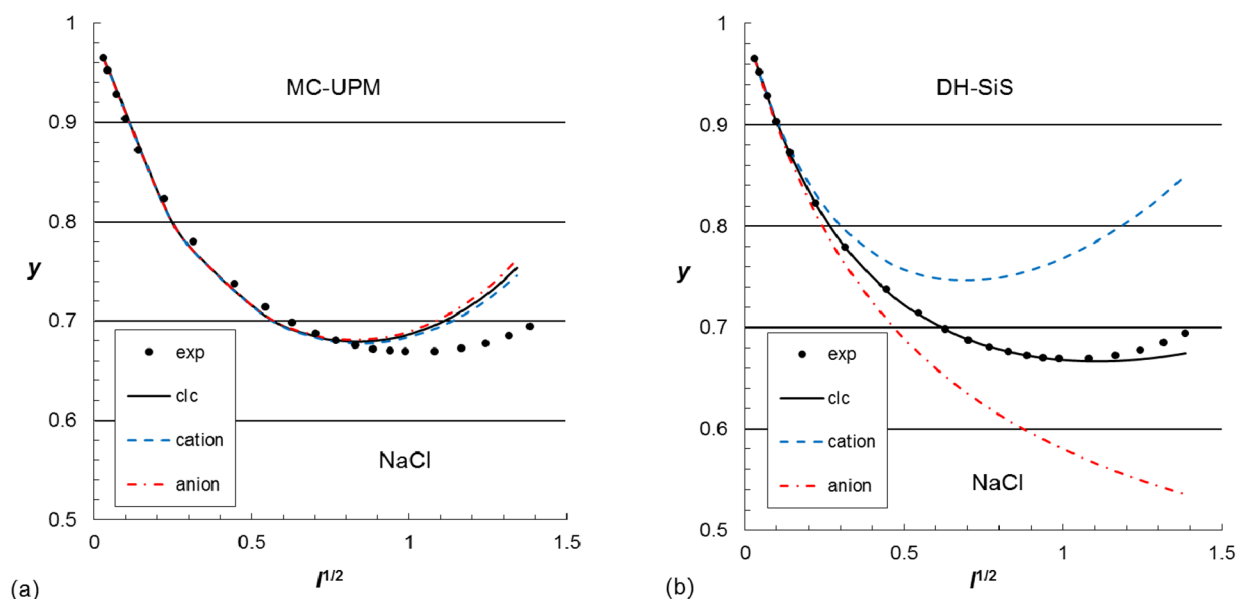
**2.3. Criteria for the Concentration Range of “Good Fit”.** The criterion chosen<sup>6</sup> for MC–UPM for the concentration range of “good fit” was  $|\ln y_{\pm}^{\text{cl}} - \ln y_{\pm}^{\text{exp}}| \leq 0.04$ . In DH–SiS, I have usually adopted a more stringent criterion for the goodness of the fit—a difference between  $\gamma_{\pm}^{\text{cl}}$  (or  $y_{\pm}^{\text{cl}}$ ) and  $\gamma_{\pm}^{\text{exp}}$  ( $y_{\pm}^{\text{exp}}$ ) not exceeding 1%. This criterion is better than that of MC–UPM because it is constant on a *relative* basis, and it is usually in accord with the experimental accuracy limit; a constant logarithmic difference limit of 0.04, as chosen in ref 6, results in a very high relative difference for small  $\gamma_{\pm}$  values, which goes far beyond the accuracy limit of the experiment. For example, with the DH–SiS computation of the best-fit  $\gamma_{\pm}^{\text{cl}}$ , NaCl exhibits <1% error up to 1.8  $m$ . With MC–UPM, the



Table 1. Ion-Size Parameters (ISPs)<sup>a</sup> of the MC–UPM and DH–SiS Fits of  $y_{\pm}$  vs  $M$ 

family	electrolyte	MC–UPM					DH–SiS					
		$b_+$	$b_-^b$	$a$	$d/2$	fit limit, M	$b_+^b$	$b_-^b$	$a$	$d/2$	% nonadditivity	fit limit, M
1–1	NaCl	336	362	349	0	0.96	194	362	352.6	74.6	26.8	1.5
1–1	KCl	270	362	316	0	0.78	266	362	355.6	41.6	13.2	1.2
1–1	NaClO <sub>4</sub>	204	480	342	0	0.49	194	480	353.5	16.5	4.9	1.5
2–1	CaCl <sub>2</sub>	548	362	455	0	0.80	198	362	339.0	59.0	21.1	1.0
2–1	Ca(ClO <sub>4</sub> ) <sub>2</sub>	530	480	505	0	1.10	198	480	388.0	49.0	14.5	0.8
3–1	LaCl <sub>3</sub>	640	362	501	0	0.97	212	362	325.6	38.6	13.4	1.0

<sup>a</sup>In pm. <sup>b</sup>Equal to the crystallographic diameters<sup>23</sup> (see also ref 1, p 37, Ahrens scale), i.e.,  $b_+ = d_+$ , and  $b_- = d_-$ ; the value for ClO<sub>4</sub><sup>−</sup> is the thermochemical diameter.<sup>1,23b</sup>



**Figure 3.** Theory–experiment fit for aqueous NaCl at 25 °C—Activity coefficient vs ionic strength: (a) MC–UPM, (b) DH–SiS. All data are in the MM system. For ISPs, see Table 1. Symbols (black filled circles) are experimental data of  $y_{\pm}$ , black full lines are of computed  $y_{\pm}$ , blue dashed broken lines are of computed  $y_+$ , and red dashed-dotted broken lines are of computed  $y_-$ .

concentration limit of good fit is claimed to be 0.96 M. That means that if  $\ln y_{\pm}^{\text{clc}}$  may be 0.04 units larger than  $\ln y_{\pm}^{\text{exp}}$ , that is,  $-0.380$  at 1 M ( $m$ ), or  $0.684$  vs  $0.657$  in  $y_{\pm}$  terms, and the experimental error is in the  $\pm 0.002$  range, this deviation would still be considered as “good fit”, but it is a 4% error, about an order of magnitude larger than the error in the DH–SiS fit. In reality, at 0.9 M, MC–UPM gives for NaCl a  $y_{\pm}$  error of 2%, corresponding to 0.02 in the  $\ln y_{\pm}$  difference; the same error occurs for NaClO<sub>4</sub> at  $\sim 0.65$  M. In the DH–SiS case, such a deviation occurs for NaCl at  $m = 2.4(!)$ , and for NaClO<sub>4</sub> at  $m = 4(!)$ ; but this deviation is considered, for DH–SiS, as being outside the concentration range of good fit.

Clearly, the criterion for good fit as chosen in ref 6 is arbitrary, only serving to afford a visually reasonable “fit” over an acceptable fit range; but when comparing different models, one should usually elect the more stringent good-fit criterion (here, that of DH–SiS). Otherwise, as done in the present work, a visual judgment of computed  $y_{\pm}$ -vs- $I$  functions by different models can be used in examining theory against experiment for fit range and quality.

### 3. RESULTS

MC–UPM and DH–SiS have been examined for six simple binary electrolytes of the 1–1, 2–1, and 3–1 valence families, which are good representatives of their respective family

members. The results are presented as computed and experimental activity coefficients against ionic strength. The DH–SiS computation has been performed using eqs 7–9, and the best-fit ISPs of DH–SiS in the MM system are listed in Table 1. The parallel MC–UPM computations and their corresponding ISPs, as given in ref 6, are also presented in Table 1 to ease their comparison with those of DH–SiS. [The ISP notations (see section 2.2) are the same for both models.]

#### 3.1. The 1–1 Electrolytes NaCl, KCl, and NaClO<sub>4</sub>

**3.1.1. NaCl and KCl.** Figures 3 (for NaCl) and 4 (KCl) present computed and experimental  $y_{\pm}$  against ionic strength (here,  $I_v = M$ ). In both cases, MC–UPM [Figures 3(a) and 4(a)] misses the experimental  $y_{\pm}$  from below up to  $I \approx 0.5$  but then crosses the experimental  $y_{\pm}$  and ascends strongly away from it. The best-fit  $b_+$  of KCl is about equal to the crystallographic diameter ( $d_+$ ) of K<sup>+</sup>, whereas  $b_+$  of NaCl is much larger than  $d_+$  of Na<sup>+</sup>. The fit is gained with  $y_- > y_+$ , and with  $y_+$  and  $y_-$  being close to each other and passing a minimum at  $I < 1$ . By visual inspection of Figures 3(a) and 4(a), the  $y_{\pm}$  fit of MC–UPM is unsatisfactory. In contrast with MC–UPM, DH–SiS gives an excellent fit at least up to  $I \approx 1$  [Figures 3(b) and 4(b)]; computed  $y_{\pm}$  values then start declining from the experimental values. The DH–SiS best fit is achieved with  $b_+ = d_+$  for both NaCl and KCl and with a nonadditive  $a$ ; the nonadditivity factor,  $d$ , is larger for the chloride with the smaller cation.

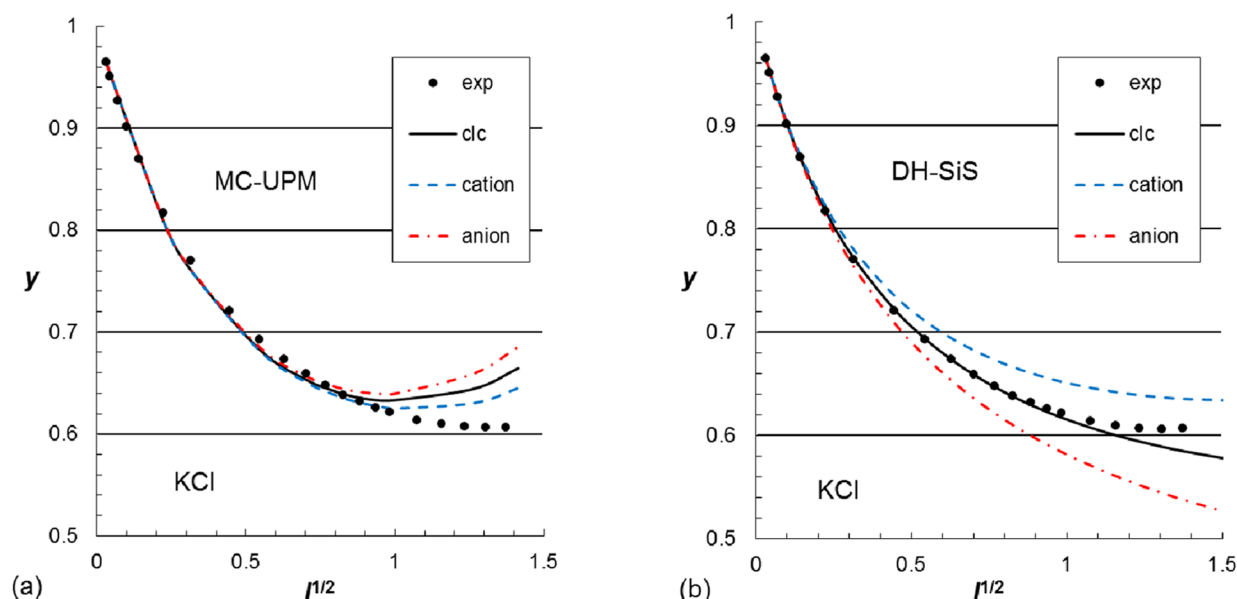
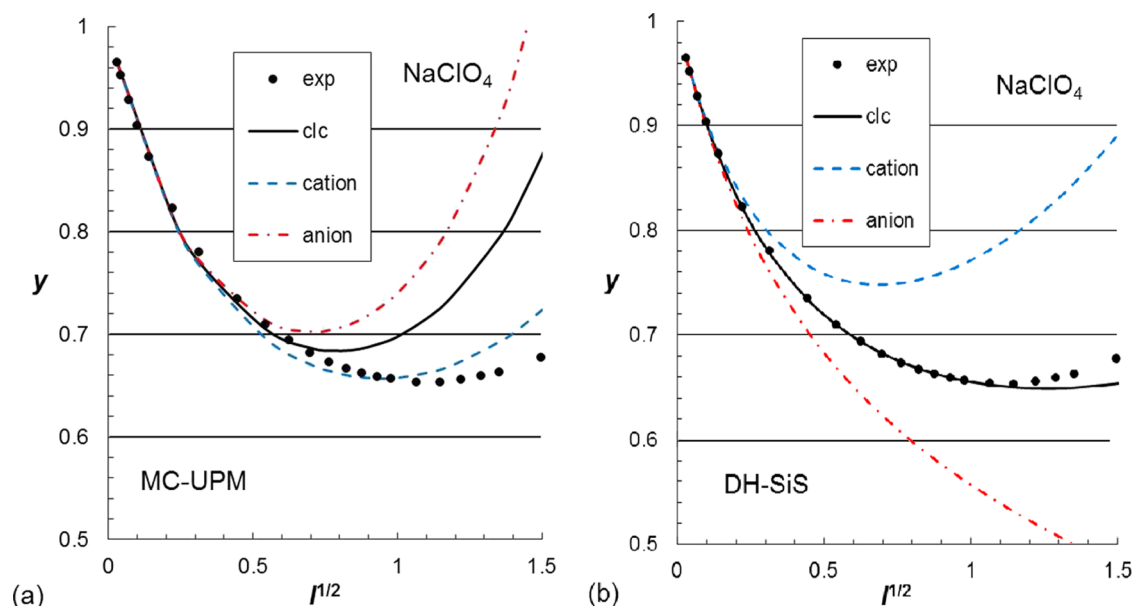


Figure 4. Same as Figure 3, for KCl.

Figure 5. Same as Figure 3, for NaClO<sub>4</sub>.

Unlike MC-UPM, DH-SiS predicts the size order  $y_+ > y_-$ ; the computed  $y_-$  is similar for both NaCl and KCl, decreasing monotonically with increase in ionic strength;  $y_+$  goes through a minimum at  $I \approx 0.5$  for NaCl but does not reach a minimum for KCl over the entire fit range. The disagreement between MC-UPM and DH-SiS on the trend and behavior of the single-ion  $y$ 's is obvious (see also below), and it stems primarily from the differences between the two models on the nature of the repulsion effect and its contribution to the various types of activity coefficients.

It is very significant that the DH-SiS prediction of  $\gamma_{\text{Na}^+}$  and  $\gamma_{\text{Cl}^-}$  for NaCl [Figure 3(b)] is in very good agreement with experimental estimates of Zhuo et al.<sup>24</sup> and of Wilczek-Vera et al.,<sup>25</sup> as demonstrated recently (Figure 1 in ref 22); the parallel MC-UPM predictions are in complete disagreement with the estimates. Appendix B provides a similar comparison for HCl. The KCl behavior presents a special case, as shown and discussed in Appendix C.

**3.1.2. NaClO<sub>4</sub>.** Sodium perchlorate is unique and deserves special attention, as explained below. Figure 5 presents computed and experimental  $y_{\pm}$  of NaClO<sub>4</sub> against ionic strength. In both MC-UPM and DH-SiS, the ClO<sub>4</sub><sup>-</sup> diameter is 480 pm; ISPs are additive for MC-UPM and almost so for DH-SiS (Table 1). Also, the MC-UPM's  $b_+$ , 204 pm (much smaller than that of the halides,<sup>6</sup> 336 pm; Table 1), is close to the crystallographic value as used in the DH-SiS fit, 194 pm. Thus, in the NaClO<sub>4</sub> case, MC-UPM and DH-SiS give best fit with experiment with almost the same ISPs! Therefore, beside the fundamental difference in predicting the single-ion activities, the two models differ from each other only in their fit range and fit quality of  $y_{\pm}$  vs  $I$ . One notices the following:

(i) The MC-UPM fit is limited to 0.5 M, but the DH-SiS fit extends to 1.5 M (Table 1); in the former case, ion association is invoked<sup>6</sup> above 0.5 M – without an independent proof – but no explanation is offered for the fact

that ion association does not occur, for example, in the case of  $\text{Ca}(\text{ClO}_4)_2$  (see below) up to  $1.1 \text{ M}^6$  – the range of “good fit”.

(ii) The DH–SiS fit quality is excellent, the average absolute deviation of theory from experiment – as  $|y_{\pm}^{\text{clc}} - y_{\pm}^{\text{exp}}|$  – being 0.0012 up to  $1.5 \text{ M}$ , far better than the parallel MC–UPM average deviation up to  $0.5 \text{ M}$ , 0.025.

The average ion size of  $337 \text{ pm}$  for  $\text{NaClO}_4$  in the DH–SiS fit [as  $(b_+ + b_-)/2$ , Table 1], raises a question why a core effect is not observed even at  $M \approx 1.5$  [Figure 5(b)]. A plausible explanation is as follows. The PM assumes that ions are hard spheres. The perchlorate ion has an effective diameter of  $480 \text{ pm}$ , but being a tetrahedral arrangement of four oxygen atoms around a Cl central atom (as formally the tiny  $\text{Cl}^{7+}$ ), this ion, when colliding with another co-ion, has a collision front of an effective size as dictated by the size of an oxygen atom (as formally  $\text{O}^{2-}$ ) in the perchlorate structure. This is illustrated schematically in the drawings of Figure 6. In all drawings, gray

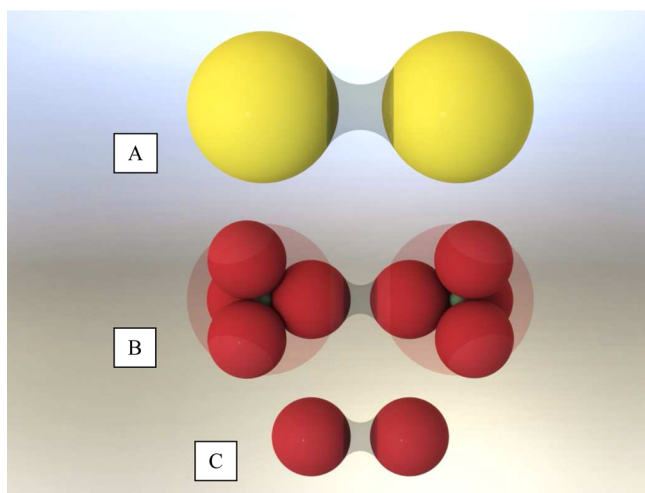


**Figure 6.** Comparison of the  $\text{ClO}_4^-$  ion with its hard sphere analog (see text). A – two hypothetical monatomic ions of the effective size of  $\text{ClO}_4^-$  approaching each other. B – two  $\text{ClO}_4^-$  ions approaching each other in the “O atom–to–O atom” mode. C – two free  $\text{O}^{2-}$  ions approaching each other.

connecting shapes represent approximate “collision spaces” of two closely approaching ionic structures. In drawing B, two  $\text{ClO}_4^-$  ions (oxygen atoms represented by red spheres, chloride atoms by green spheres) are approaching each other. The dispersive forces are in fact not between the whole structures but between two oxygen atoms of the tetrahedral arrangement in  $\text{ClO}_4^-$ . This is similar to the nonelectrostatic hard-sphere interaction between two approaching “free”  $\text{O}^{2-}$  ions (drawing C) and much smaller compared with the same interaction when two charged hard spheres of diameter  $480 \text{ pm}$ , representing a hypothetical monatomic ion somewhat larger than  $\text{I}^-$ , approach each other, as shown in drawing A (yellow spheres). As a result, the use of the effective size of the  $\text{ClO}_4^-$  anion, idealized as sphere (pale pink spheres in drawing B of Figure 6), is causing a computation of an unrealistically large core effect in the PM, as manifested in Figure 5(a). The behavior of other oxo and complex ions, including hydrated ions (see Part 2, DOI 10.1021/ct500694u), can be explained similarly.

The real core effect in  $\text{NaClO}_4$  is perhaps that occurring above  $\sim 1.5 \text{ M}$ , and its magnitude may be estimated from

the computation–experiment fit in Figure 5(b). Because MC–UPM approximates  $\text{ClO}_4^-$  as a monolithic hard sphere, fitting model-predicted activity coefficients of  $\text{NaClO}_4$  with experimental values is impossible beyond  $0.5 \text{ M}$ . The fit below  $0.5 \text{ M}$  is good because at this low concentration the core effect is small even with a large hard sphere ( $480 \text{ pm}$ ) as representative of the perchlorate ion. At  $<0.1 \text{ M}$ , where both the core effect and the net-SiS-derived electrostatic repulsion effects are very small, the PM effectively merges with the DH model. With each of the ISPs being practically the same in the MC–UPM and the DH–SiS computation (see above), this indirectly justifies the simplifications made in DH–SiS (i.e., the concept of ionic atmosphere, the use of the linearized PB equation, etc.). This is so since at  $<0.1 \text{ M}$ , DH–SiS and MC–UPM give essentially the same electrostatic excess functions, but in the latter model, considered statistical-mechanically rigorous, the electrostatic interactions are computed without the above simplifications.

Overall, even by visual inspection of Figure 5(a), but more so when examining the figure numerically and graphically (not shown), the shape of the UPM-predicted  $y_{\pm}$ -vs- $I^{1/2}$  curve is inadequate for the actual behavior of  $\text{NaClO}_4$  over the entire concentration range of the fit. This is similar to the cases of other 1–1 electrolytes. It seems that reducing the  $|y_{\pm}^{\text{clc}} - y_{\pm}^{\text{exp}}|$  deviation at small concentration is achievable with further adjustment of the cation size upward, while losing more fit range; this casts doubt on the physicality of the cation size of best fit in MC–UPM (see Part 2, DOI 10.1021/ct500694u). Because a larger cation size causes a smaller concentration range of good fit, the explanation given by Abbas et al.<sup>6</sup> for the deviation of MC–UPM from experiment implies that a higher hydration state of the cation causes a higher degree of ion association, but this is counterintuitive. For example, for  $\text{AlCl}_3$  and  $\text{LaCl}_3$ , with recommended cationic diameters interpreted as those of ions with two sheaths of water molecules surrounding them,<sup>6</sup> the fit is good even at  $M = 1$ ,<sup>6</sup> or  $I = 6$ , meaning that ion association is not indicated up to this fit limit. This is in spite of the fact that at any given concentration,  $\text{AlCl}_3$  and  $\text{LaCl}_3$  ionize in solution to twice the number of ions of ionized  $\text{NaClO}_4$ . Thus, one has to conclude that something very basic is wrong or missing either in the MC simulation method of Abbas et al.<sup>6</sup> or in the PM itself.

The pattern of the overall behavior of  $y_+$  and  $y_-$  in MC–UPM and DH–SiS, as depicted in Figure 5, is similar to that of the 1–1 chlorides (Figures 3 and 4), but due to the much larger size of the perchlorate ion, the size difference between  $y_+$  and  $y_-$  is far greater in  $\text{NaClO}_4$  than in the chlorides. This emanates straightforwardly from the very nature of each of the two models of the current comparison. No experimental estimate of  $\gamma_{\text{Na}^+}$  and/or  $\gamma_{\text{ClO}_4^-}$  (or the corresponding  $y$ 's) as a function of concentration seems to currently exist for  $\text{NaClO}_4$ ; but the similarity between  $\text{NaClO}_4$  (Figure 5) and  $\text{NaCl}$  (Figure 3) suggests parallel experimental trends of the single-ion activities, and, therefore, predicted values of DH–SiS [Figure 5(b)] should be correct and those of MC–UPM [Figure 5(a)] should not.

**3.1.3. Differences between Computed and Experimental  $y_{\pm}$ .** For better differentiation between the two models of the current comparison, in terms of fit quality and fit range, Figure 7 presents, for  $\text{NaCl}$ , the percent deviation of computed  $y_{\pm}$  ( $y_{\pm}^{\text{clc}}$ ) from experimental  $y_{\pm}$  ( $y_{\pm}^{\text{exp}}$ ) as a function of concentration.  $\% \Delta y_{\pm}$  is defined as  $100(y_{\pm}^{\text{clc}} - y_{\pm}^{\text{exp}})/y_{\pm}^{\text{exp}}$ . The behavior of  $\text{KCl}$  and  $\text{NaClO}_4$  (not shown) is very similar to that of  $\text{NaCl}$ , and

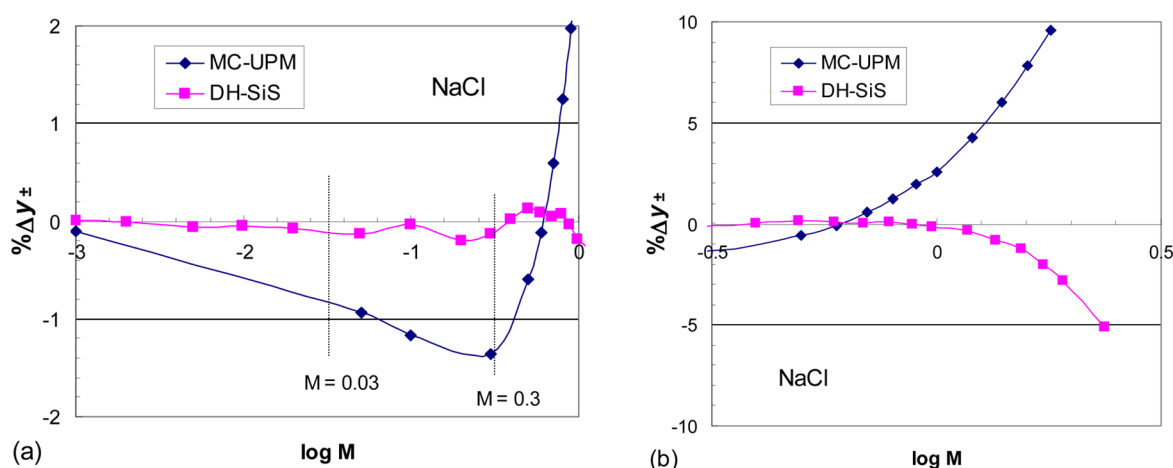


Figure 7. Percent deviation of  $y_{\pm}^{\text{clc}}$  from  $y_{\pm}^{\text{exp}}$ ,  $\% \Delta y_{\pm}$ , for NaCl: (a) extended molar range, (b) high molarity.

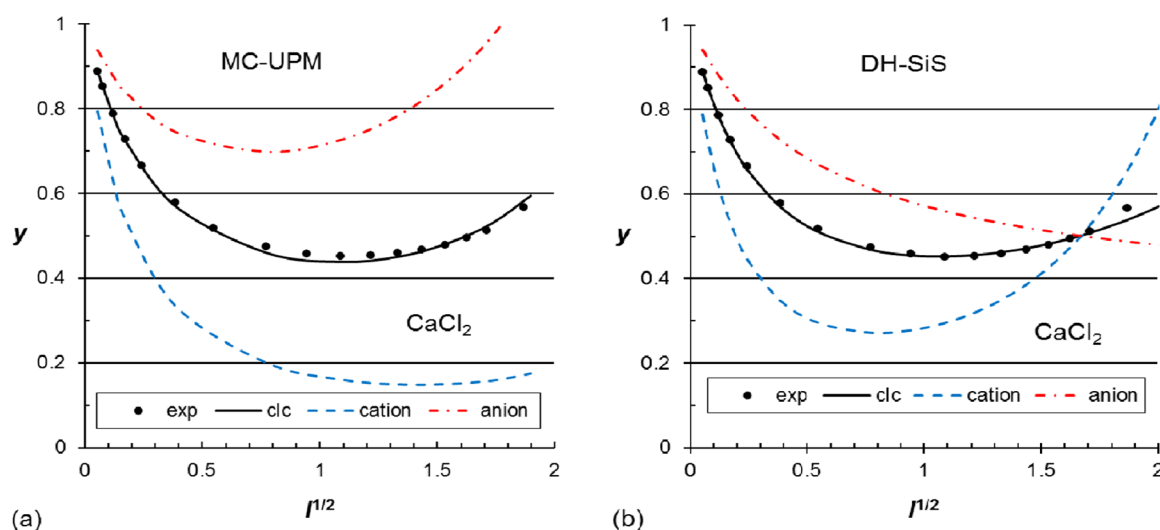


Figure 8. Same as Figure 3, for  $\text{CaCl}_2$ .

therefore Figure 7 depicts the general trend of the simple 1–1 electrolytes. In all three cases, MC–UPM initially exhibits a considerable negative deviation from experiment, which becomes greater with increasing  $M$ ; the extent of deviation then reaches a maximum (minimum in  $\% \Delta y_{\pm}$ ), changes course, turns smaller, crosses the experimental data (i.e., changes sign from negative to positive at  $\Delta y_{\pm} = 0$ ), and eventually increases strongly at high electrolyte concentration. Clearly, as mentioned earlier, this indicates that MC–UPM is unsatisfactory for 1–1 electrolytes, and it reflects a major failure of the PM, which is fully revealed by the study of Abbas et al.<sup>6</sup> In contrast with MC–UPM, DH–SiS gives a very reasonable (i.e., small)  $\% \Delta y_{\pm}$  (Figure 7) that does not exhibit a systematic trend and prevails over the entire range of concentration of good fit.

**3.2. The 2–1 Electrolytes  $\text{CaCl}_2$  and  $\text{Ca}(\text{ClO}_4)_2$ .** When comparing 2–1 electrolytes with 1–1 electrolytes, it is of advantage to keep the crystallographic diameters<sup>23</sup> of the cation ( $d_+$ ) and anion ( $d_-$ ) – thus, the parameters  $b_+$  and  $b_-$  – about the same in both cases; then, besides the somewhat varying counterion contact distance, the two electrolyte types differ from each other only in the cation valence that changes from 1 to 2. I, therefore, have chosen to compare  $\text{CaCl}_2$  with NaCl and  $\text{Ca}(\text{ClO}_4)_2$  with  $\text{NaClO}_4$ . The two sets of electrolytes have two very different  $d_-$  ( $= b_-$ ) values. Consequently, in this comparison,

one may expect to mainly see the difference in electrolyte behavior due to the change in valence family from 1–1 to 2–1 at two different  $b_-$  values. The cases of calcium chloride and calcium perchlorate are presented in Figures 8 and 9, respectively.

With the two 2–1 electrolyte systems, the fit is good for both MC–UPM and DH–SiS, even though  $y_+$  and  $y_-$  are, as expected, very different between the two models. As in the case of 1–1 electrolytes,  $y_+$  and  $y_-$  in MC–UPM have similar trends, and they both go through a minimum and follow a parallel pattern of nonintersecting curves over the entire  $I$  range. In DH–SiS, only  $y_+$  has a minimum, and it is deeper compared with that of  $y_+$  in MC–UPM, which is shallow and occurring at higher concentration. In the DH–SiS analysis,  $y_+$  is much lower in  $\text{CaCl}_2$  than in NaCl, but the minimum occurs at the same  $I$  value; also, the minimum  $\log y_+$  value of  $\text{CaCl}_2$  is four times smaller than that of NaCl. This follows straightforwardly from the effect of  $z_+$  (as  $z_+^2$ ) on  $y_+$  (or  $\gamma_+$ ) (see eq 7), and from the lack of influence of  $z_+$  on the value of  $I$  at the minimum in  $y_+$  ( $\gamma_+$ ), when all other factors remain the same, as has been discussed before.<sup>7</sup> The same behavior is seen when comparing  $\text{Ca}(\text{ClO}_4)_2$  with  $\text{NaClO}_4$ . Unlike the change in  $y_+$ , the monotonic decline in  $y_-$  is about the same for the two chlorides and for the two perchlorates as dictated by the SiS model and its mathematical workup:



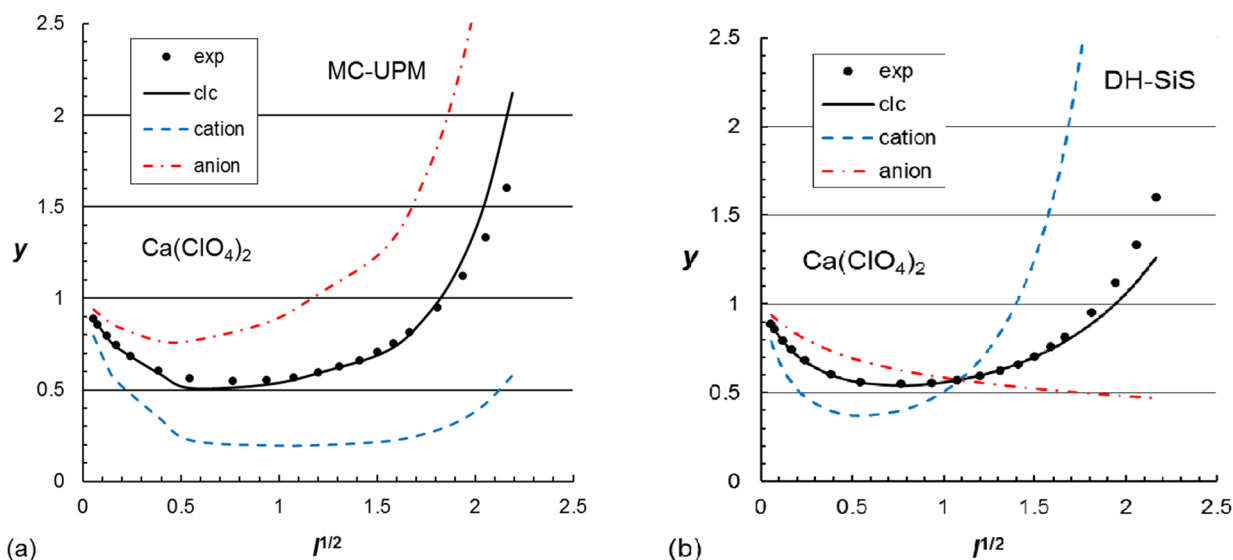


Figure 9. Same as Figure 3, for  $\text{Ca}(\text{ClO}_4)_2$ .

$$y_{\text{Cl}^-}(\text{NaCl}) \approx y_{\text{Cl}^-}(\text{CaCl}_2) \text{ and } y_{\text{ClO}_4^-}(\text{NaClO}_4) \approx y_{\text{ClO}_4^-}(\text{Ca}(\text{ClO}_4)_2)$$

In MC-UPM, over the entire fit range, there is almost no difference between  $y_+$  and  $y_-$  in NaCl [Figure 3(a)] but a very large difference in  $\text{CaCl}_2$  [Figure 8(a)]. This is especially due to the much smaller  $y_+$  value in the latter electrolyte, which partially reflects the effect of  $z_+$  in the  $y_+$ -vs- $I^{1/2}$  function. The core effect in  $y_+$  of  $\text{CaCl}_2$  is not very strong compared to that in  $y_+$  of NaCl even though the MC-UPM's best fit is achieved with the size of the (hydrated)  $\text{Ca}^{2+}$  ion in  $\text{CaCl}_2$  being much larger than the size of the (hydrated)  $\text{Na}^+$  ion in NaCl.<sup>6</sup> In MC-UPM, there is more disparity between  $y_+$  and  $y_-$  in  $\text{NaClO}_4$  [Figure 5(a)] than in NaCl [Figure 3(a)], but the  $y_+$ - $y_-$  difference is still wider in  $\text{Ca}(\text{ClO}_4)_2$  [Figure 9(a)]; the differences between  $y_+$  and  $y_-$ , when going from  $\text{NaClO}_4$  to  $\text{Ca}(\text{ClO}_4)_2$ , and from NaCl to  $\text{CaCl}_2$ , are of similar nature.

A major difference between MC-UPM and DH-SiS is in the interrelation between  $y_+$  and  $y_-$ . In both models, at low  $I$ ,  $y_+ < y_-$ , but in the DH-SiS case, a strong increase in  $y_+$  past its minimum causes a crossover of its curve with that of  $y_-$  so there is an  $I$  value at which  $y_+ = y_- = y_{\pm}$ , and then, at higher  $I$ ,  $y_+ > y_-$ . Indeed, the experimental estimate of the single-ion activities in  $\text{CaCl}_2$ , as reported by Wilczek-Vera et al.,<sup>25</sup> corroborates the DH-SiS prediction [Figure 8(b)] while contrasting with the prediction of MC-UPM [Figure 8(a)]; see Figure 4 in ref 22. A similar behavior is found for  $\text{MgCl}_2$  (Figure 3 in ref 22). No experimental estimate of  $y_+$  and  $y_-$  for  $\text{Ca}(\text{ClO}_4)_2$  seems available yet.

Another major difference between MC-UPM and DH-SiS in the 2-1 calcium electrolytes is that for DH-SiS,  $b_+$  is equal to the crystallographic diameter of  $\text{Ca}^{2+}$ , hence it reflects a naked  $\text{Ca}^{2+}$  ion; but for MC-UPM,  $b_+$  has a very large value that can be reconciled only with hydrated  $\text{Ca}^{2+}$ . The relative ISP nonadditivity in DH-SiS (not existing in MC-UPM) is similar between  $\text{CaCl}_2$  and NaCl (~20%, Table 1) but somewhat different between the perchlorates of calcium and sodium.

The 2-1 electrolytes of the present comparison exhibit a similar behavior of  $\% \Delta y_{\pm}$  vs  $M$ , as depicted for  $\text{CaCl}_2$  in Figure 10. They qualitatively follow the 1-1 behavior (Figure 7), but both MC-UPM and DH-SiS have the same fit quality up to 0.05 M. The computed data initially deviate negatively from experiment but then, at higher concentration — >0.3 M — change course,

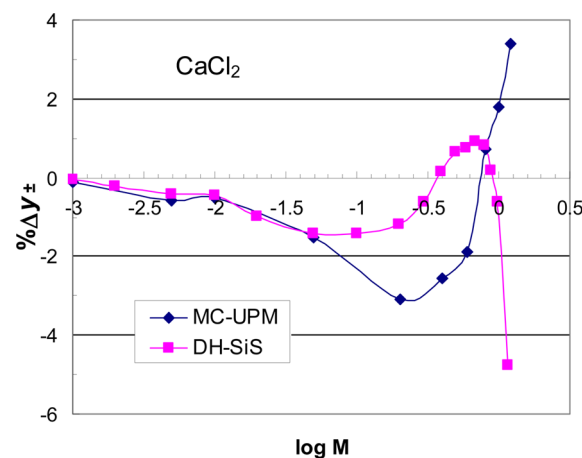
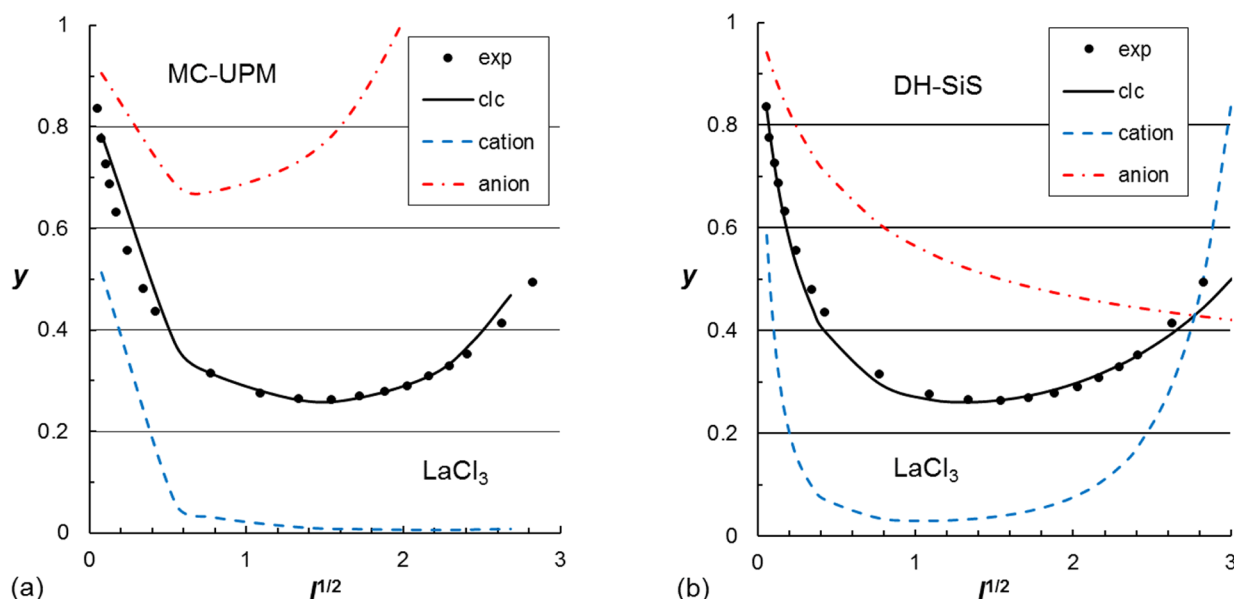


Figure 10. Percent deviation of  $y_{\pm}^{\text{calc}}$  from  $y_{\pm}^{\text{exp}}$ ,  $\% \Delta y_{\pm}$ , for  $\text{CaCl}_2$ .

starting to exhibit a positive deviation. At last, when approaching 1 M, a strong positive deviation occurs with MC-UPM, whereas DH-SiS deviates from experiment very negatively. In the concentration midrange of ~0.05–0.8 M,  $\% \Delta y_{\pm}$  is smaller for DH-SiS than for MC-UPM, reflecting a better suitability of DH-SiS in representing 2-1 electrolytes. Both MC-UPM and DH-SiS give larger  $\% \Delta y_{\pm}$  values in the 2-1 electrolytes than in the 1-1 electrolytes. Thus, the fit quality of both models is overall poorer for this higher-valence electrolyte family.

**3.3. The 3-1 Electrolyte  $\text{LaCl}_3$ .** For the above reasons in the comparison of 2-1 calcium electrolytes with 1-1 sodium electrolytes, comparing the 3-1 electrolyte system with the 2-1 and 1-1 systems can be conveniently done with lanthanum chloride being contrasted with the chlorides of calcium and sodium. This is because apart from all three electrolytes sharing the same anion, the crystallographic sizes of  $\text{La}^{3+}$ ,  $\text{Ca}^{2+}$ , and  $\text{Na}^+$  are very similar (Table 1). Figure 11 presents the  $\text{LaCl}_3$  case.

As in the calcium electrolytes in section 3.2, the fit range and fit quality for both MC-UPM [Figure 11(a)] and DH-SiS [Figure 11(b)] are about the same, and the main difference is in  $y_+$  and  $y_-$ . In MC-UPM,  $y_-$  goes through a sharp minimum at  $I \approx 0.35$ , and  $y_+$  declines to about 0 at  $I \approx 1$  and remains so at higher  $I$ . In the DH-SiS analysis,  $y_-$  declines monotonically over the entire fit range and is similar in value to  $y_-$  in NaCl



**Figure 11.** Same as Figure 3, for  $\text{LaCl}_3$ .<sup>26</sup> [Lines in (a) are not curved at low  $I$  due to lack of sufficient MC computation data.]

and  $\text{CaCl}_2$ . However,  $y_+$  declines very sharply to a minimum of  $\sim 0.01$  (at  $I \approx 1$ ) and then rises strongly, especially above  $I = 4$ , crossing the  $y_-$  curve, as in the case of 2–1 electrolytes (see above), at a point where  $y_+ = y_- = y_{\pm}$ ; this point is somewhat above the  $I$  limit of good fit. The  $\text{LaCl}_3$  behavior agrees with the essence of the SiS treatment as pointed out previously (see comparison between  $\text{NaCl}$ ,  $\text{CoCl}_2$ , and  $\text{NdCl}_3$ , on the LR scale, in ref 7).

In  $\text{LaCl}_3$ ,  $\% \Delta y_{\pm}$  vs  $M$  (Figure 12) follows the general trend of 1–1 and 2–1 electrolytes, but two differences are noticed:

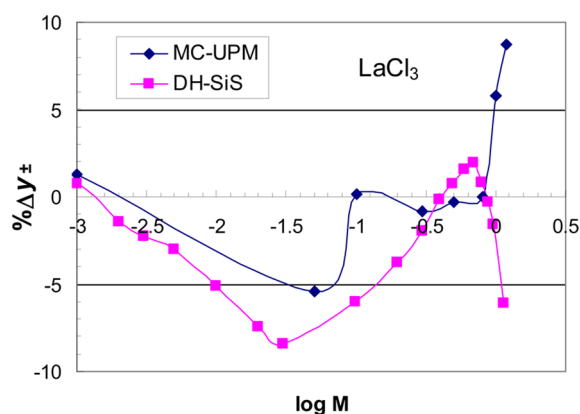


**Figure 12.** Same as Figure 10, for  $\text{LaCl}_3$ .

First, overall, DH–SiS deviates from experiment more strongly than MC–UPM; second, with the latter model, the fit is especially good in the concentration range of 0.1–0.8 M. Nonetheless, the two computational methods are of about the same effectiveness (see Figure 11) considering the inconsistencies in the reported experimental  $\gamma_{\pm}$  data of  $\text{LaCl}_3$  (compare data in ref 10, p 502 with those in ref 11, p 566).

A previous comparison<sup>7</sup> between MC simulation of the RPM in the 3–1 system (with  $R = 420$  pm) and parallel SiS computation (with  $a = b_+ = b_- = 420$  pm, on the LR scale) has demonstrated that a very good agreement exists between the two methods up to  $\sim 0.4$  M. The current comparison is of “best fits” for  $\text{LaCl}_3$ , based on ISP adjustments in the UPM realm:

DH–SiS uses the crystallographic sizes of both  $\text{La}^{3+}$  and  $\text{Cl}^-$ , and the best fit is achieved with a somewhat elongated counterion closest distance (a), deviating 13% from ISP additivity (Table 1); MC–UPM’s best fit is achieved<sup>6</sup> with a whopping  $\text{La}^{3+}$  “diameter” of 640 pm and, consequently, a large  $a$  value, 500 pm. A 640-pm positively charged multimolecular spherical entity in aqueous solution, composed of an aggregate of mostly water molecules weakly held through coordination bonding, cannot behave as “hard sphere” according to the definition of the PM (see Part 2, DOI 10.1021/ct500694u); nor could it provide a core potential (due to dispersive forces between electron clouds) similar to that of a hypothetical monatomic anion with  $d_- = 640$  pm. Therefore, even though the MC–UPM fit for  $\text{LaCl}_3$  is fair, it is achieved with ISPs of questionable validity.

#### 4. DISCUSSION

Most advanced theories of electrolyte solutions that have been developed over the past five decades are based on the primitive model (PM).<sup>2</sup> The old DH theory has been claimed<sup>27</sup> to also be founded on the PM but wrongly neglecting the interaction potential between atmospheric ions, the exclusion volume of these ions, and the hard-sphere potential. It is more appropriate, however, to regard the DH theory as a “non-PM theory” despite its parallel to theories based on the restricted PM (RPM). DH–SiS, a development of an “unrestricted” DH model, is analogous to the unrestricted PM (UPM), but the two models cannot be equated.

Advanced integral equation theories have always been judged for their accuracy by comparing their predicted excess thermodynamic functions with those obtained by simulations of the PM, in most cases, the RPM. The HNC equation,<sup>19</sup> various versions of the Modified Poisson–Boltzmann (MPB) equation,<sup>28</sup> and to a lesser extent the Mean Spherical Approximation (MSA) equation<sup>29–31</sup> have been indeed found to agree with MC simulations of the PM. But is the PM an adequate model for real-life electrolytes? The recent work of Abbas et al.<sup>6</sup> is allowing, for the first time, a critical evaluation of the PM concept and its suitability for actual ionic solutions.

Note that regardless of whether the PM is suitable or not for electrolytes in nature, this model is, in fact, unphysical since it assumes that the core potential is discontinuous at  $r = R_{ij}$ .<sup>2,17,18</sup> It is thus strange that PM-based theories, e.g., HNC, have been claimed physically accurate and statistical-mechanically rigorous. In practice, the PM still reasonably approximates the physics of electrolyte solutions, especially if the nonelectrostatic repulsion potential is chosen as the repulsion component of the Lennard-Jones (L-J) potential, that is, decaying as  $r^{-n}$ , e.g., with  $n = 12$ . However, the L-J potential is not a good description of actual molecular (and ionic) collisions<sup>32</sup> but rather a convenient mathematical form for the overall dispersive attraction–repulsion effect. A potential with smaller  $n$ , e.g., 9 (as in Friedman's calculations;<sup>17</sup> see also Appendix B in the subsequent Part 2, DOI 10.1021/ct500694u), seems more adequate, allowing extended decay of the dispersive repulsion effect over a broader  $r$  range. Even better, the repulsion function may be approximated as an exponential decay.<sup>32</sup> However, in the current analysis I have accepted the PM for what it is by definition, ignoring its unphysicality. My focus has been on comparing two *highly simplified* models, the PM and the ion atmosphere (DH) model (Figure 2), for their *relative* effectiveness in representing real ionic solutions.

In the present work, I have compared computations of activity coefficients of a selected group of electrolytes by both MC–UPM (the UPM simulated by a MC method<sup>6</sup>) and DH–SiS (the “unrestricted Debye–Hückel” type SiS treatment). The major comparison has been of computed  $\gamma_{\pm}$  against experimental  $\gamma_{\pm}$  (converted from the parallel  $\gamma_{\pm}$ ).  $\gamma_{\pm}$  ( $\gamma_{\pm}$  is a solid thermodynamic excess function. A secondary comparison has involved the single-ion activity coefficients  $\gamma_{+}$  and  $\gamma_{-}$  for which reliable experimental estimates are available in a few cases (as  $\gamma_{+}$ ,  $\gamma_{-}$ ). In most compared cases, especially of 1–1 electrolytes, the DH–SiS computation–experiment fit of  $\gamma_{\pm}$  has been found considerably better than the MC–UPM fit: (1) Its overall quality is better, (2) It extends to higher ionic strength, and (3) It employs the crystallographic or thermochemical sizes of both cations and anions (as thoroughly discussed in Part 2, DOI 10.1021/ct500694u). Furthermore, as I have recently reported,<sup>22</sup> the predicted single-ion activity coefficients ( $\gamma_i$ 's) of DH–SiS are in harmony with parallel activity coefficients estimated from experiment, whereas those of MC–UPM are at odds with the estimate.

An important factor in assessing ionic theories is the actual effect of the hard sphere potential. Hydration and ion association arguments are frequently related directly to the excessive role that is usually attributed to this core repulsion potential in the PM. But this potential may be mostly contributing in monatomic ions of  $n$ –1 electrolytes ( $n = 1, 2, 3$ ). In contrast, a core effect appears missing in essentially all other electrolyte valence families, and – not surprisingly – those families were *not* analyzed by Abbas et al.<sup>6</sup> Real electrolytes of such families (e.g., 1–2, 1–3, 1–4, 3–2) typically do not exhibit minima in excess functions plotted against ionic strength;<sup>7</sup> furthermore, such families commonly involve large di- and polyvalent anions (e.g.,  $\text{SO}_4^{2-}$ ,  $\text{PO}_4^{3-}$ ,  $[\text{Fe}(\text{CN})_6]^{3-}$ ), and therefore, MC–UPM would have to exhibit a minimum in the activity coefficient (or osmotic coefficient) vs concentration (or ionic strength), followed by a strong increase of this function beyond the minimum. The only way to apply a MC–UPM analysis on those systems is to resort to ion association arguments and extend them down to very low electrolyte concentrations. Thus, to mask the failure of the PM in the above cases, one should invoke, without proof, limited electrolyte dissociation at

concentrations at which those system are otherwise considered “strong”, that is, fully ionized (e.g., in calculating their  $\gamma_{\pm}$  from electrochemical potentials). In this manner, the analysis would practically avoid a core contribution, but then the PM would be reduced to a purely electrostatic model. The UPM would then offer no advantage over the simple SiS model, and RPM would not provide more physical insight into electrolyte solutions beyond the DH model.

In closing, even though Abbas et al.<sup>6</sup> did a very important, long-overdue study on the fit between the PM and experiment, the present study demonstrates that their conclusion that their results prove the physical validity of the PM is inconsistent with their factual findings that prove, instead, *the opposite*: As representative of real electrolyte solutions, the PM is imperfect and flawed, if not straightforwardly wrong.

## 5. CONCLUSION

The present study and its outcome can be summarized as follows.

1. Computational predictions of the *mean ionic activity coefficient* of strong electrolyte solutions as a function of ionic strength, optimized against literature experimental data, have been compared between two methods: (a) simulations of the primitive model (PM), and (b) the Smaller-ion Shell (SiS) treatment.

2. The  $\gamma_{\pm}$  computations of Abbas et al.<sup>6</sup> by Monte Carlo (MC) simulation of the unrestricted PM (UPM) (here, “MC–UPM”), have been confronted with parallel computations using the analytic mathematical expression of SiS (“DH–SiS”),<sup>7,8</sup> after its conversion from the LR system ( $\gamma_{\pm}$  vs  $m$ ) to the MM system ( $\gamma_{\pm}$  vs  $M$ ).

3. The MC–UPM/DH–SiS comparison has been performed for 1–1, 2–1, and 3–1 electrolyte systems, represented by six easy-to-compare cases: NaCl, KCl,  $\text{NaClO}_4$ ,  $\text{CaCl}_2$ ,  $\text{Ca}(\text{ClO}_4)_2$ , and  $\text{LaCl}_3$ .

4. The contours of the MC–UPM's  $\gamma_{\pm}$ –vs– $I$  plots deflect from experiment, especially in the classical cases of 1–1 electrolytes. Concentration limits of the “fit” have been explained<sup>6</sup> as resulting from ion association.

5. DH–SiS plots exhibit, instead, more suitable  $\gamma_{\pm}$ –vs– $I$  contours, and the fit ranges are usually broader than those of MC–UPM.

6. Furthermore, unlike MC–UPM, DH–SiS achieves best fit with experiment through employing co-ion ISPs that are equal to the respective crystallographic diameters and do not change for different counterions.

7. Consequently, the current work concludes that the involvement of core (hard-sphere), hydration (in general, solvation), and ion-pairing (ion association) effects in the nonideality of electrolyte solutions, as reflected by excess functions, are less pronounced in reality than hitherto thought; at least, this is so at electrolyte concentration below about 1 M.

## ■ APPENDIX A

### Conversion of Activity Coefficient *versus* Concentration From the LR to the MM Scale

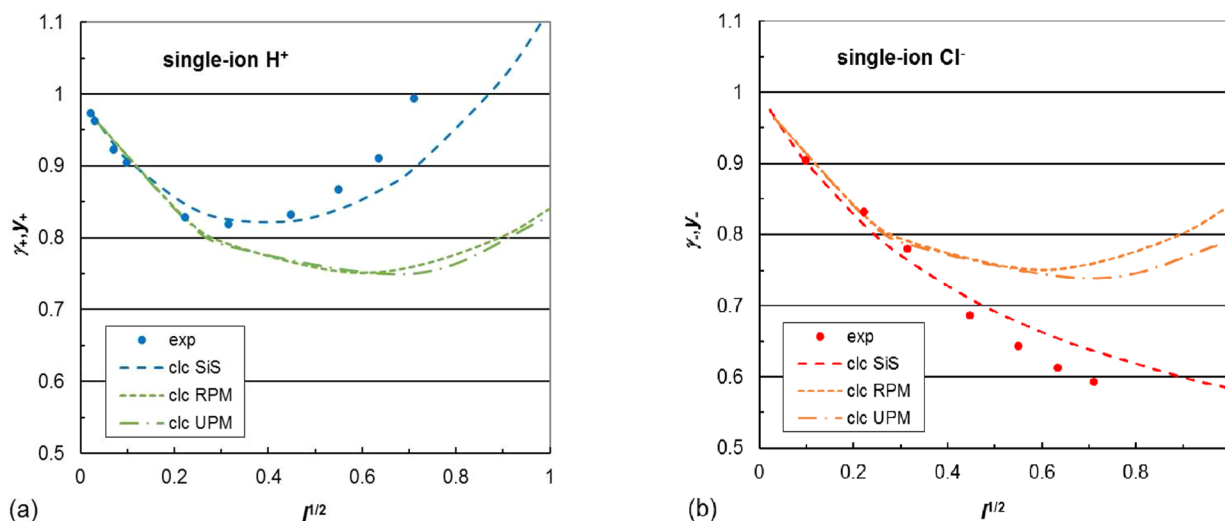
This Appendix is a supplement for assisting readers in navigating between activity coefficients in the LR and MM scale, for all six electrolytes of the present study. The conversion of  $m$  to  $C(M)$  and experimental  $\gamma_{\pm}$  to  $\gamma_{\pm}$  has been performed following Abbas et al.<sup>33</sup> (see also chapter 2 in ref 10), using their eq 23

Table A1. Activity Coefficients of the Six Electrolytes of the Present Study, in the LR and MM Scales<sup>a</sup>

<i>m</i>	NaCl, <i>A</i> = 0.6938			KCl, <i>A</i> = 0.6327			NaClO <sub>4</sub> , <i>A</i> = 0.6835			CaCl <sub>2</sub> , <i>A</i> = 0.8214			Ca(ClO <sub>4</sub> ) <sub>2</sub> , <i>A</i> = 0.7285			LaCl <sub>3</sub> , <i>A</i> = 0.9711		
	<i>m</i>	<i>M</i>	$\gamma_{\pm}$	<i>m</i>	<i>M</i>	$\gamma_{\pm}$	<i>m</i>	<i>M</i>	$\gamma_{\pm}$	<i>m</i>	<i>M</i>	$\gamma_{\pm}$	<i>m</i>	<i>M</i>	$\gamma_{\pm}$	<i>m</i>	<i>M</i>	$\gamma_{\pm}$
0.001	0.0010	0.965	0.9650	0.001	0.0010	0.965	0.001	0.0010	0.965	0.001	0.0010	0.888	0.001	0.0010	0.888	0.0005	0.0005	0.835
0.002	0.0020	0.952	0.9520	0.002	0.0020	0.951	0.002	0.0020	0.952	0.002	0.0020	0.851	0.002	0.0020	0.857	0.0010	0.0010	0.776
0.005	0.0050	0.928	0.9281	0.005	0.0050	0.927	0.005	0.0050	0.928	0.005	0.0050	0.787	0.005	0.0050	0.793	0.0020	0.0020	0.726
0.01	0.0100	0.903	0.9032	0.01	0.0100	0.901	0.01	0.0100	0.903	0.01	0.0100	0.727	0.01	0.0100	0.741	0.0030	0.0030	0.687
0.02	0.0199	0.872	0.8723	0.02	0.0199	0.869	0.02	0.0199	0.872	0.02	0.0199	0.664	0.02	0.0199	0.680	0.0050	0.0050	0.631
0.05	0.0498	0.822	0.8227	0.05	0.0498	0.816	0.05	0.0498	0.821	0.05	0.0498	0.577	0.05	0.0497	0.603	0.0100	0.0100	0.556
0.1	0.0995	0.778	0.7794	0.1	0.0994	0.768	0.1	0.0993	0.777	0.1	0.0995	0.517	0.1	0.0990	0.557	0.0200	0.0200	0.480
0.2	0.1987	0.735	0.7377	0.2	0.1983	0.717	0.2	0.1978	0.729	0.2	0.1986	0.472	0.2	0.1967	0.540	0.0300	0.0300	0.436
0.3	0.2975	0.710	0.7139	0.3	0.2966	0.687	0.3	0.2956	0.701	0.3	0.2972	0.455	0.3	0.2930	0.540	0.0512	0.1	0.0996
0.4	0.3959	0.693	0.6980	0.4	0.3944	0.666	0.4	0.3925	0.683	0.4	0.3954	0.448	0.4	0.3879	0.552	0.05675	0.2	0.1989
0.5	0.4940	0.681	0.6872	0.5	0.4917	0.650	0.5	0.4887	0.668	0.5	0.4932	0.448	0.5	0.4813	0.573	0.05935	0.3	0.2978
0.6	0.5917	0.673	0.6804	0.6	0.5883	0.637	0.6	0.5840	0.657	0.6	0.5904	0.453	0.6	0.5733	0.598	0.06241	0.4	0.3961
0.7	0.6890	0.667	0.6756	0.7	0.6845	0.626	0.7	0.6785	0.648	0.7	0.6871	0.460	0.7	0.6637	0.627	0.06593	0.5	0.4938
0.8	0.7860	0.662	0.6718	0.8	0.7800	0.618	0.8	0.7722	0.641	0.8	0.7833	0.470	0.8	0.7527	0.664	0.07037	0.6	0.5907
0.9	0.8826	0.659	0.6700	0.9	0.8750	0.610	0.9	0.8650	0.635	0.9	0.8790	0.484	0.9	0.8401	0.706	0.07541	0.7	0.6868
1	0.9788	0.657	0.6693	1	0.9695	0.604	0.6212	1	0.9570	0.630	0.6563	1	0.9742	0.500	0.5117	0.8	0.7819	0.302
1.2	1.1701	0.654	0.6688	1.2	1.1568	0.593	0.6133	1.2	1.1386	0.622	0.6536	1.2	1.1629	0.550	0.5659	0.9	0.8762	0.321
1.4	1.3598	0.655	0.6724	1.4	1.3418	0.586	0.6096	1.4	1.3170	0.616	0.6529	1.4	1.3493	0.599	0.6197	1	0.9694	0.342
1.6	1.5480	0.657	0.6771	1.6	1.5247	0.580	0.6069	1.6	1.4920	0.613	0.6554	1.6	1.5334	0.657	0.6835	1.2	1.1528	0.398
1.8	1.7347	0.662	0.6849	1.8	1.7053	0.576	0.6062	1.8	1.6638	0.611	0.6591	1.8	1.7151	0.726	0.7597	1.4	1.3318	0.470
2	1.9199	0.668	0.6938	2	1.8838	0.573	0.6065	2	1.8324	0.609	0.6628					1.6	1.5063	0.561

<sup>a</sup>Experimental  $\gamma_{\pm}$ -vs-*m* data are from ref 10 and references cited in ref 7; for LaCl<sub>3</sub>, see footnote 26. *A* is the constant in eq A1; see ref 33.





**Figure B1.** Single-ion activity coefficients as functions of ionic strength for  $\text{H}^+$  (a) and  $\text{Cl}^-$  (b) of HCl in water at 25 °C. The activity coefficients are  $\gamma_+$  and  $\gamma_-$  for the experiment<sup>34</sup> and the SiS calculation; they are  $\gamma_+$  and  $\gamma_-$  for the PM. (Since the concentration range of interest is  $<1\text{ m}$ , parallel  $\gamma$  and  $\gamma$  values are not very different, so no LR  $\rightarrow$  MM conversion is necessary considering the required accuracy for the comparison as given in the figure.) Symbols (full circles; blue for  $\text{H}^+$ , red for  $\text{Cl}^-$ ) are experimental data. Lines (broken; blue for  $\text{H}^+$ , red for  $\text{Cl}^-$ ) are of the computed behavior, as specified in the figure insets.

$$\ln \sigma_{\text{sol}} = \ln \sigma_0 + \frac{AmW}{mW + 1000} \quad (\text{A1})$$

where  $\sigma_{\text{sol}}$  is the solution density, and  $\sigma_0$  is the solvent (here, water) density, both at 25 °C (as  $\text{g}/\text{cm}^3$ );  $W$  is the molecular weight of the solute, and  $A$ , an empirical factor.  $A$  for each electrolyte has been adopted from Table 2 of ref 33. The molarity ( $C$ , in M units) is calculated from molality using eq 22 of ref 33

$$C = \frac{1000m\sigma_{\text{sol}}}{1000 + mW} \quad (\text{A2})$$

and the molar activity coefficient relates to the molal coefficient through

$$\gamma_{\pm} = \gamma_{\pm} \frac{m\sigma_0}{C} = \gamma_{\pm} \frac{\sigma_0}{\sigma_{\text{sol}}} \left( 1 + \frac{mW}{1000} \right) \quad (\text{A3})$$

Table A1 lists, for the six electrolytes of the present work, the  $\gamma_{\pm}$ -vs- $m$  literature data and their corresponding  $\gamma_{\pm}$ -vs- $M$  data.

## ■ APPENDIX B

### Single-Ion Activity Coefficients in Aqueous HCl: Experiment versus Predictions of MC-RPM, MC-UPM, and DH-SiS

Sakaida and Kakiuchi have recently reported<sup>34</sup> an experimental determination of the single-ion activity coefficients of  $\text{H}^+$  and  $\text{Cl}^-$  in aqueous HCl solution, by electrochemical measurements in the concentration range 0.0005–0.5  $m$ . They performed their measurements in a Harned cell in which they installed a specially designed ionic liquid salt bridge having a very stable liquid junction potential and ion-selective electrodes for  $\text{H}^+$  and  $\text{Cl}^-$ . In other experimental studies of individual ion activities of HCl solutions, researchers determined the activity of one ion and calculated the activity of the counterion using experimental values of the mean ionic activity (e.g., ref 25). Unlike those studies, Sakaida and Kakiuchi measured the single-ion electrochemical potentials for  $\text{H}^+$  and  $\text{Cl}^-$  separately and independently and then calculated the corresponding  $\gamma_{\text{H}^+}$  and  $\gamma_{\text{Cl}^-}$ . From the  $\gamma_i$ 's, they have calculated  $\gamma_{\pm}$  values and shown their agreement with values measured experimentally from the entire cell

potential. Furthermore, Sakaida and Kakiuchi have pointed out that their results are in accord with predictions of the SiS equations. Here I extend the above comparison by including in it the computation of the PM. For this, I use the optimized RPM and UPM predictions<sup>6</sup> of  $\gamma_{\text{H}^+}$  and  $\gamma_{\text{Cl}^-}$  in HCl solutions. The results are depicted in Figure B1.

Single-ion activity coefficients of  $\text{H}^+$  and  $\text{Cl}^-$  against ionic strength are presented in Figure B1(a) and Figure B1(b), respectively. The experiment-derived data are compared with the predictions of the SiS model and of the PM model. Indeed, there is a good general agreement between the experiment and the SiS prediction for both  $\text{H}^+$  and  $\text{Cl}^-$  up to moderate concentration. At more concentrated solution, the experiment gives higher  $\gamma_{\text{H}^+}$  and lower  $\gamma_{\text{Cl}^-}$  values than the prediction, but the trends of experiment and theory (SiS) are clearly similar: In both sets of data there is a minimum in  $\gamma_{\text{H}^+}$ , which occurs at about the same concentration, and a monotonic decline in  $\gamma_{\text{Cl}^-}$  without reaching or approaching a minimum throughout the entire concentration range of the comparison.

In contrast with both experiment and DH-SiS, the optimized curves of MC-RPM and MC-UPM exhibit a totally different behavior of  $\gamma_{\text{H}^+}$  and  $\gamma_{\text{Cl}^-}$ : While agreeing quite well between themselves, past  $\sim 0.05\text{ I}$ , the two PM fits give a considerably smaller  $\gamma_{\text{H}^+}$  that goes through a minimum at much higher concentration ( $\sim 0.3$  instead of  $\sim 0.12\text{ m}$ ); past  $\sim 0.1\text{ I}$ , the PM fits give a far larger  $\gamma_{\text{Cl}^-}$  than the estimate, which also goes through a minimum (again at  $\sim 0.3\text{ m}$ ). Over the entire concentration range of interest of the present comparison,  $\gamma_{\text{H}^+} > \gamma_{\text{Cl}^-}$  for the experimental estimate and for DH-SiS, but  $\gamma_{\text{H}^+} \approx \gamma_{\text{Cl}^-}$  for MC-RPM and MC-UPM.

The strong disagreement between single-ion activity coefficients of aqueous HCl predicted by MC-RPM/MC-UPM, and the  $\gamma_{\text{H}^+}$  and  $\gamma_{\text{Cl}^-}$  values of Sakaida and Kakiuchi, indicates that MC simulations of the PM do not produce adequate single-ion activity values. The adjusted ISPs of the PM, giving “best fit” in the HCl case,<sup>6</sup> are 413 pm for the RPM (as “ $a$ ”) and 440 pm for the diameter of  $\text{H}^+$  in the UPM (for which the chloride diameter is chosen as the crystallographic value, and the ISPs are additive). The size of the proton (as

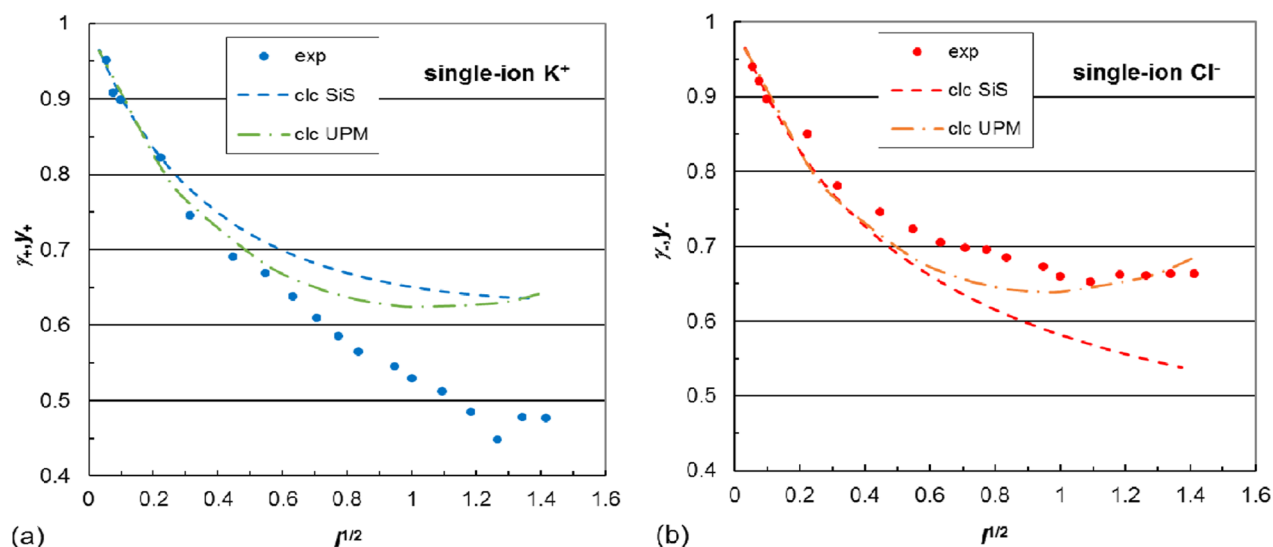


**Figure C1.** Same as Figure B1, for KCl (i.e., with  $K^+$  replacing  $H^+$ ). Experimental data are from ref 25.

$H_3O^+$ ) is strongly exaggerated in the fits of ref 6, and albeit claimed to represent a hydrated proton, it cannot be considered as a genuine physical quantity; the extended size of  $H^+$  only serves to force a “best fit” of PM-derived  $\gamma_{\pm}$  values<sup>6</sup> with the experimental  $\gamma_{\pm}$  values of aqueous HCl. Even then, the fit limit of MC-UPM (1.92 M) is smaller than that of DH-SiS (3.0 M) (see more on this in Part 2, DOI 10.1021/ct500694u).

## ■ APPENDIX C

### Single-Ion Activity Coefficients in Aqueous KCl: Experiment versus Predictions of MC-UPM and DH-SiS

Experimental estimates of the individual ion activity coefficients of KCl solutions (in water at 25 °C) are provided in Wilczek-Vera et al.<sup>25</sup> Because those estimates are not in agreement with DH-SiS, this Appendix is devoted to a full-scale comparison of the experiment with the prediction of both DH-SiS and MC-UPM. The results are shown – in Figure C1 – in a parallel manner to those of HCl in Appendix B (Figure B1). Figure C1(a) is for  $K^+$ , and Figure C1(b) is for  $Cl^-$ . It is immediately noticed that  $Cl^-$  behaves in the experiment differently than expected based on Figure B1(b) (for HCl) as well as Figure 2 of ref 22 (for LiCl) and Figure 1 of ref 22 (for NaCl).

In the experiment, the single-ion activity coefficients of  $Cl^-$  in the  $I$  range  $\sim 0.1$ – $0.9$  are considerably larger than the values predicted by DH-SiS and by MC-UPM. Above  $I \approx 0.9$ , the experiment is closer to the prediction of MC-UPM, but this is deceiving since the MC-UPM curve is definitely of a different nature than the experimental trend: The curve goes through a clear minimum at  $I \approx 1$  and then rises significantly; the experiment shows a general trend of decline over the entire ion strength range, eventually leveling off above  $I \approx 1$ . The experiment is very close to the MC-UPM curve at high  $I$  (however, see below), but at lower  $I$ , the MC-UPM curve tends to be closer to the DH-SiS curve than to the experiment.

The “agreement” between DH-SiS and MC-UPM is definitely “better” for  $K^+$  [Figure C1(a)], and both models disagree sharply with the experimental estimate, especially above  $I = 0.3$ . Past this ion strength, the experiment exhibits a strong monotonic decline of the  $K^+$  activity. DH-SiS also predicts a monotonic decline, but its values are much larger than those of the estimate. MC-UPM again, as in the  $Cl^-$  case,

predicts a minimum at  $I \approx 1$ . As before, (e.g., the HCl case), MC-UPM predicts  $\gamma_{+} \approx \gamma_{-}$ .

Note that the comparison above  $I \approx 1$  is of compromised quality since the fit limit of MC-UPM is only  $\sim 0.9$  (as  $I^{1/2}$ ) and that of DH-SiS is  $\sim 1.1$ . For MC-UPM, up to the fit limit the agreement with DH-SiS is “better” than the agreement with the experimental estimate for both  $K^+$  and  $Cl^-$ . It should also be pointed out that, strangely, within the above  $I$  range of good fit, the DH-SiS-predicted curve for  $K^+$  agrees quite well with the estimated  $\gamma_{Cl^-}$  curve, and the DH-SiS-predicted curve for  $Cl^-$  reasonably follows the estimated  $\gamma_{K^+}$  curve.

Overall, this odd behavior of KCl is of a disagreement between the two models, on the one hand, and the experimental estimate, on the other hand. This theory–experiment inconsistency is a puzzle, and one may blame either the experiment or the theory (both models) or both. The fact that KCl solutions behave differently than NaCl solutions in the dissolution of simple amino acids<sup>35</sup> and that the activity coefficients of solutions of alanine (but *not* of serine) respond differently to the presence of NaCl and KCl<sup>36</sup> may indicate some “anomaly” in KCl; but how this can be translated to differences between single-ion activities of NaCl and KCl is unclear. There is definitely a need for more experimental and theoretical study on the electrolyte nature of KCl in solution.

### Nomenclature

The nomenclature of this article is combined with that of Part 2 (subsequent article, DOI 10.1021/ct500694u).

## ■ AUTHOR INFORMATION

### Corresponding Author

\*E-mail: dfraenkel@eltronresearch.com.

### Notes

The authors declare no competing financial interest.

## ■ REFERENCES

- (1) Barthel, J. M. G.; Krienke, H.; Kunz, W. *Physical Chemistry of Electrolyte Solutions, Topics in Physical Chemistry 5*; Steinkoppf: Darmstadt, 1998.
- (2) Friedman, H. L. *J. Chem. Phys.* **1960**, *32*, 1134.
- (3) Bopp, P. *The Physics and Chemistry of Aqueous Ionic Solutions*; Bellissent-Funel, M.-C., Neilson, G. W., Eds.; Reidel Publishing Company: Dordrecht, 1987; p 217.

- (4) Turk, P. *The Physics and Chemistry of Aqueous Ionic Solutions*, Bellissent-Funel, M.-C., Neilson, G. W., Eds.; Reidel Publishing Company: Dordrecht, 1987; p 409.
- (5) Andersen, H. C. *Modern Aspects of Electrochemistry*, No. 11; Conway, B. E., Bockris, J. O'M., Eds.; Plenum Press: New York, 1975; Chapter 1, p 1. Here, a simplified explanation is offered for the (otherwise quite complicated to grasp) essence of the effective potential according to the MM solution theory. An ion-pair correlation function,  $g_{ij}^{\circ}(r)$  can be defined for the hypothetical case of two ions,  $i$  and  $j$ , in solution at infinite dilution, to further define an effective potential  $w_{ij}^{\circ}(r)$  as (omitting the subscripts and the reference to distance  $r$ )  $w^{\circ} = -kT \ln g^{\circ}$ .  $g^{\circ}$  and, therefore,  $w^{\circ}$  are each a lump of terms that we do not wish to explicitly consider, including the influence of the solvent, hydration of ions, dielectric effects, etc. Under certain conditions, the properties of a real solution (finite concentration) can be calculated as if it were a dilute "gas of ions", but this requires the use of the effective potential as defined above and *not* the real potential.
- (6) Abbas, Z.; Ahlberg, E.; Nordholm, S. *J. Phys. Chem. B* **2009**, *113*, 5905.
- (7) Fraenkel, D. *Mol. Phys.* **2010**, *108*, 1435.
- (8) Fraenkel, D. *J. Phys. Chem. B* **2011**, *115*, 557.
- (9) Debye, P.; Hückel, E. *Phys. Z.* **1923**, *24*, 185.
- (10) Robinson, R. A.; Stokes, R. H. *Electrolyte Solutions*, 2nd ed.; Butterworths: London, 1959.
- (11) Harned, H. S.; Owen, B. B. *The Physical Chemistry of Electrolytic Solutions*, 3rd ed.; Reinhold Publishing Corp.: New York, 1958.
- (12) Davidson, N. *Statistical Mechanics*; McGraw-Hill: New York, 1962; Chapter 21.
- (13) Bockris, J. O'M.; Reddy, A. K. N. *Modern Electrochemistry*, Vol. 1, 2nd ed.; Plenum Press: New York, 1998; Chapter 3; also 1st ed.; 1970; Chapter 3.
- (14) Hansen, J. P. *The Physics and Chemistry of Aqueous Ionic Solutions*, Bellissent-Funel, M.-C., Neilson, G. W., Eds.; Reidel Publishing Company: Dordrecht, 1987; p 1.
- (15) McMillan, W. G., Jr.; Mayer, J. E. *J. Chem. Phys.* **1945**, *13*, 276.
- (16) Mayer, J. E. *J. Chem. Phys.* **1950**, *18*, 1426.
- (17) Friedman, H. L. *Modern Aspects of Electrochemistry* No. 6; Bockris, J. O'M., Conway, B. E., Eds.; Plenum Press: New York, 1971; p 1.
- (18) Friedman, H. L. *Ionic Solution Theory*; Wiley: New York, 1962.
- (19) Rasaiah, J. C.; Friedman, H. L. *J. Chem. Phys.* **1968**, *48*, 2742.
- (20) Widom, B. *J. Chem. Phys.* **1963**, *39*, 2808.
- (21) Svensson, B. R.; Woodward, C. E. *Mol. Phys.* **1988**, *64*, 247.
- (22) Fraenkel, D. *J. Phys. Chem. B* **2012**, *116*, 3603.
- (23) (a) *CRC Handbook of Chemistry and Physics*, 58th ed.; Weast, R. C., Ed.; CRC Press: Cleveland, OH, 1977–1978; F-213. (b) Marcus, Y. *Chem. Rev.* **1988**, *88*, 1475.
- (24) Zhuo, K.; Dong, W.; Wang, W.; Wang, J. *Fluid Phase Equilib.* **2008**, *274*, 80.
- (25) Wilczek-Vera, G.; Rodil, E.; Vera, J. H. *AIChE J.* **2004**, *50*, 445.
- (26) Experimental data are from the following sources: Low concentration, 0.0005–0.03 M, from Spedding, F. H.; Atkinson, G. *The Structure of Electrolyte Solutions*; Hamer, W. J., Ed.; Wiley: New York, 1959; p 319. High concentration, 0.1–1.6 m, from ref 10, p 502.
- (27) Carley, D. D. *J. Chem. Phys.* **1967**, *46*, 3783.
- (28) Martinez, M. M.; Bhuiyan, L. B.; Outhwaite, C. W. *J. Chem. Soc., Faraday Trans.* **1990**, *86*, 3383.
- (29) Triolo, R.; Grigera, J. R.; Blum, L. *J. Phys. Chem.* **1976**, *80*, 1858.
- (30) Lu, J.-F.; Yu, Y.-X.; Li, Y.-G. *Fluid Phase Equilib.* **1993**, *85*, 81.
- (31) Fawcett, W. R.; Tikanen, A. C. *J. Phys. Chem.* **1996**, *100*, 4251.
- (32) Atkins, P.; de Paula, J. *Physical Chemistry*, 9th ed.; W.H. Freeman and Company: New York, 2010; p 642.
- (33) Abbas, Z.; Gunnarsson, M.; Ahlberg, E.; Nordholm, S. *J. Phys. Chem. B* **2002**, *106*, 1403.
- (34) Sakaida, H.; Kakiuchi, T. *J. Phys. Chem. B* **2011**, *115*, 13222.
- (35) Khoshkbarchi, M. K.; Vera, J. H. *Ind. Eng. Chem. Res.* **1997**, *36*, 2445.
- (36) Khoshkbarchi, M. K.; Soto-Campos, A. M.; Vera, J. H. *J. Solution Chem.* **1997**, *26*, 941.